

## Subatomic and Astroparticles Physics Master Oral Defence

# INNOVATIVE METHODS FOR ELECTROMAGNETIC CALORIMETERS BASED ON SCINTILLATING CRYSTALS

Julie Delenne

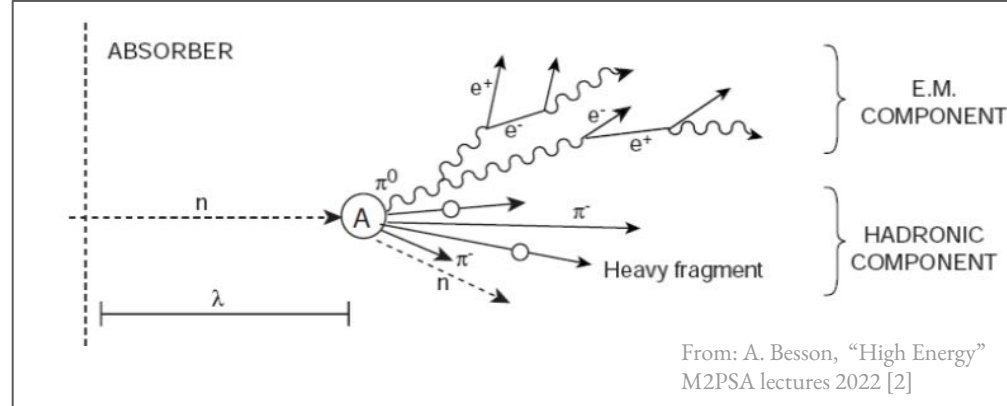
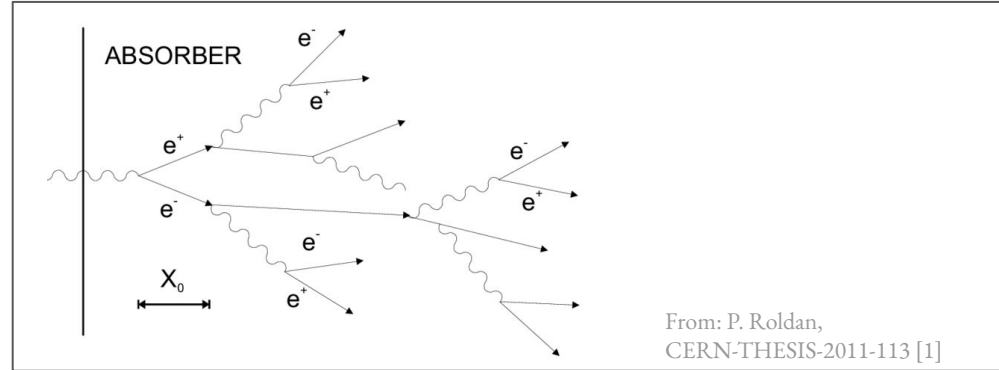
Supervisor & Co-supervisor: Etienne Auffray, Loris Martinazzoli

June 19<sup>th</sup>, 2024

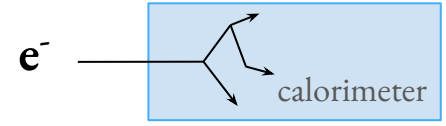
# 1. Calorimetry background

## □ Radiation-matter interaction

- High energy **electrons** → Bremsstrahlung  
High energy **photons** → Pair production  
Radiation length  $X_0$   
⇒ **electromagnetic showers.**
- High energy **hadrons** → complex interactions  
Interaction length  $\lambda$   
⇒ **hadronic showers** made of two components: **electromagnetic and hadronic components.**



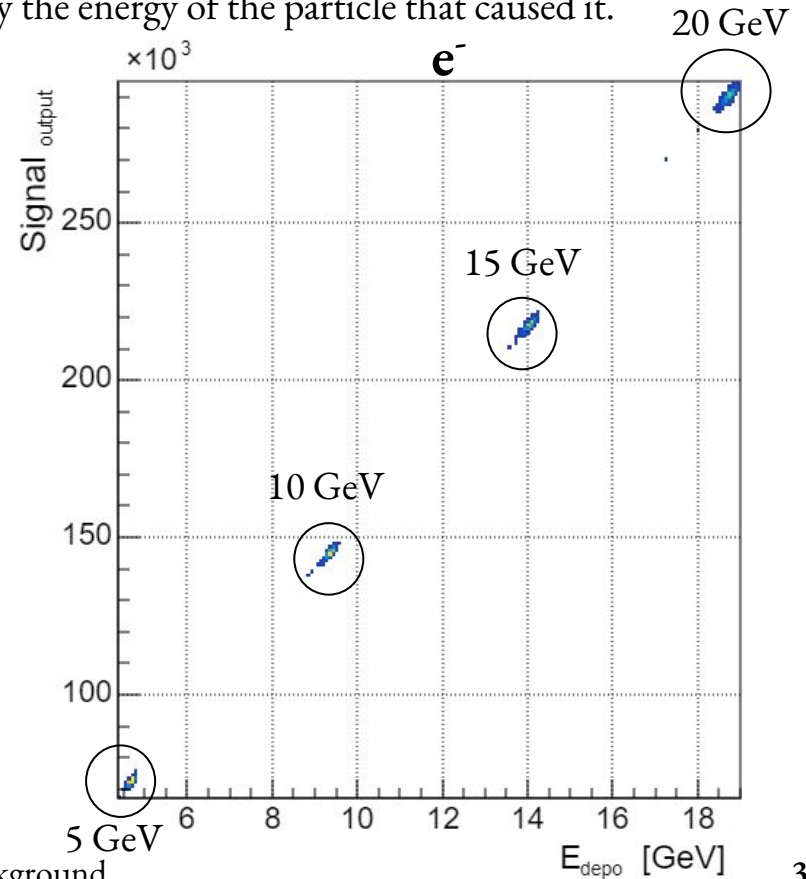
## □ Response of the calorimeter



↳ defined as the average calorimeter signal divided by the energy of the particle that caused it.

→ **Electromagnetic (e.m.) showers:**

$$\left( \frac{\text{Signal}_{\text{output}}}{E_{\text{depo}}} \right)_{e.m.} = e$$



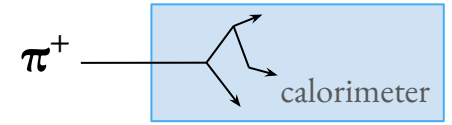
→ **Hadronic (h.)** showers:

$$\left( \frac{\text{Signal}_{\text{output}}}{E_{\text{depo}}} \right)_{h.} = \underbrace{ef_{em}}_{\text{e.m.}} + \underbrace{h(1 - f_{em})}_{\text{h.}}$$

with e, h calibration constants and  $f_{em}$ , the electromagnetic fraction of the shower (= fraction of hadron energy deposited via e.m. processes).

→ **Different responses** depending on the showers  $\Rightarrow$  Worsens energy resolution.

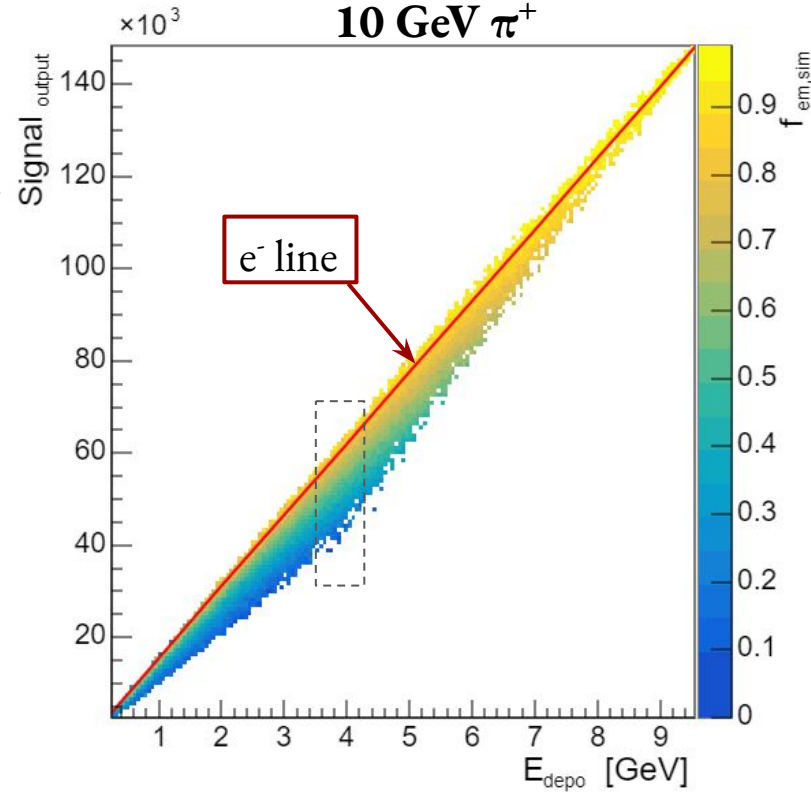
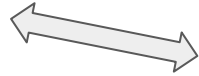
→ **Hadronic (h.) showers:**



$$\left( \frac{\text{Signal}_{\text{output}}}{E_{\text{depo}}} \right)_{h.} = \underbrace{ef_{em}}_{\text{e.m.}} + \underbrace{h(1 - f_{em})}_{\text{h.}}$$

with e, h calibration constants and  $f_{em}$ , the electromagnetic fraction of the shower (= fraction of hadron energy deposited via e.m. processes).

- **Different responses** depending on the showers  $\Rightarrow$  Worsens energy resolution.
- $f_{em}$  **fluctuates** with the energy  $\Rightarrow$  Proportionality lost in hadronic showers.



# Outlines

1. Calorimeter background
- 2. Dual-readout calorimetry**
3. Simulation
4. Pulse shape discrimination
5. Reconstruction energy
6. Conclusion & Ongoing work

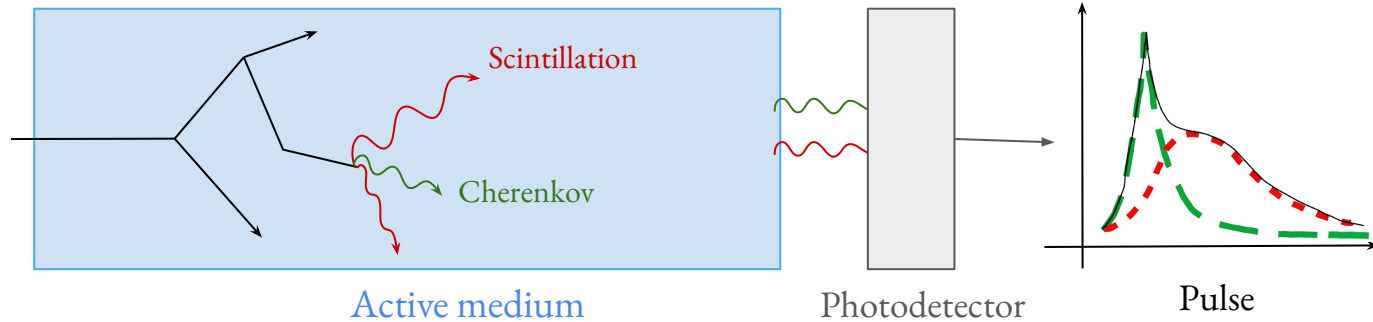
- **Homogeneous calorimeters based on scintillating crystals**

↳ High-energy particles interact with the crystals that compose the calorimeter by depositing their energy converted to photons from 2 independent processes:

→ **Scintillation** (isotropic)

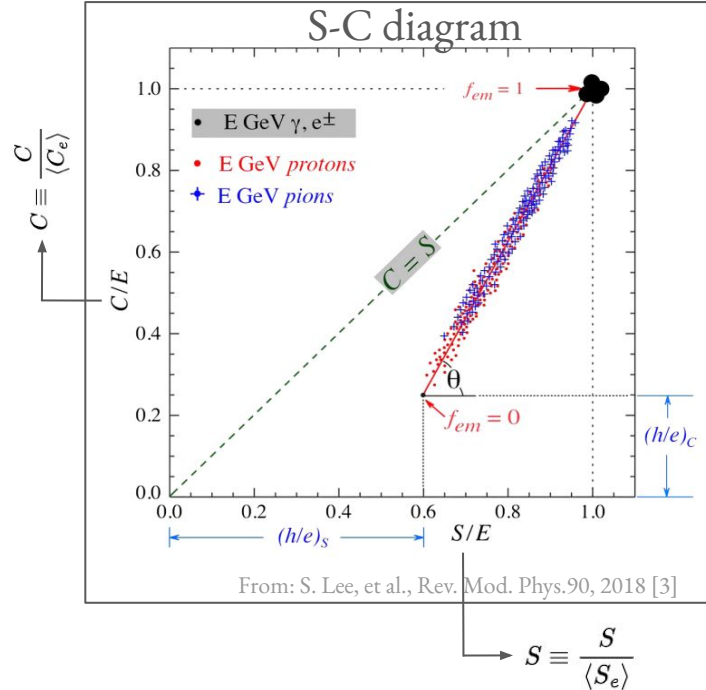
→ **Cherenkov** (directional & prompt light, mainly emitted by **e.m.** particles).

Scheme of photodetector pulse processing with calorimeters based on scintillating crystals



## 2. Dual-readout calorimetry

- Energy detection technique that improves measurement accuracy by using **two types of readings** to correct complex hadron interactions in calorimeters:
- Scintillation (**S**) signals
  - Cherenkov (**C**) signals
- Both signals can be calibrated with electrons of known E energy.

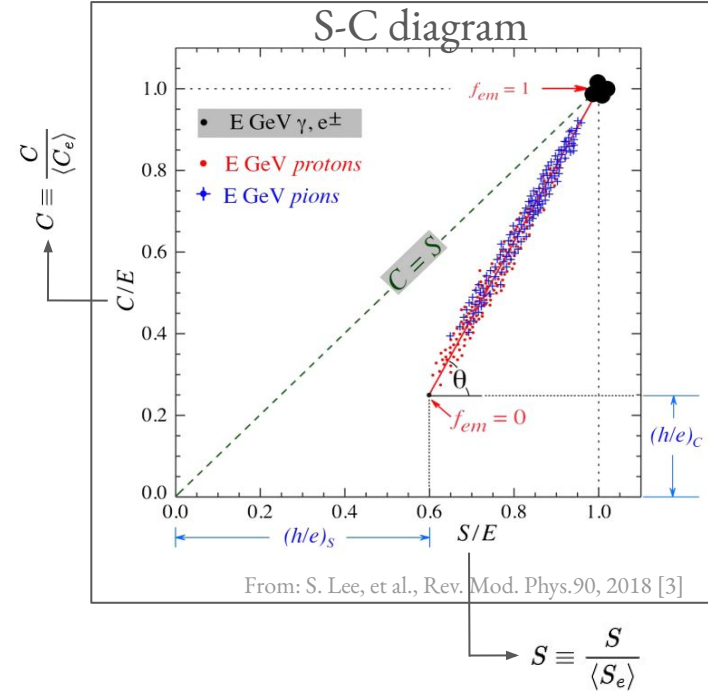




## 2. Dual-readout calorimetry

- Energy detection technique that improves measurement accuracy by using **two types of readings** to correct complex hadron interactions in calorimeters:
  - Scintillation (**S**) signals
  - Cherenkov (**C**) signals
- Both signals can be calibrated with electrons of known E energy.
- The dual-readout method works thanks to the fact that  $(\mathbf{e}/\mathbf{h})_S \neq (\mathbf{e}/\mathbf{h})_C$ . The larger the difference between both values, the better the e.m. shower fraction  $f_{em}$  can be extrapolated.

$$\begin{cases} S = E \left[ f_{em} + \frac{1}{(e/h)_S} (1 - f_{em}) \right] \\ C = E \left[ f_{em} + \frac{1}{(e/h)_C} (1 - f_{em}) \right] \end{cases}$$



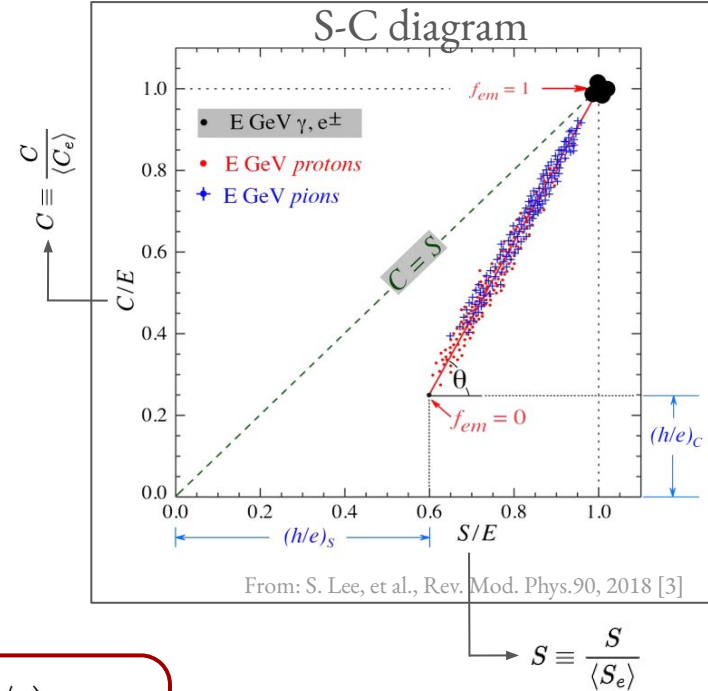
## 2. Dual-readout calorimetry

- ➔ Energy detection technique that improves measurement accuracy by using **two types of readings** to correct complex hadron interactions in calorimeters:
  - Scintillation (**S**) signals
  - Cherenkov (**C**) signals
- Both signals can be calibrated with electrons of known E energy.
- The dual-readout method works thanks to the fact that  $(\mathbf{e}/\mathbf{h})_S \neq (\mathbf{e}/\mathbf{h})_C$ . The larger the difference between both values, the better the e.m. shower fraction  $f_{em}$  can be extrapolated.

$$\begin{cases} S = E \left[ f_{em} + \frac{1}{(e/h)_S} (1 - f_{em}) \right] \\ C = E \left[ f_{em} + \frac{1}{(e/h)_C} (1 - f_{em}) \right] \end{cases}$$



$$f_{em} = \frac{(h/e)_C - (C/S)(h/e)_S}{(C/S) [1 - (h/e)_S] - [1 - (h/e)_C]}$$



## 2. Dual-readout calorimetry

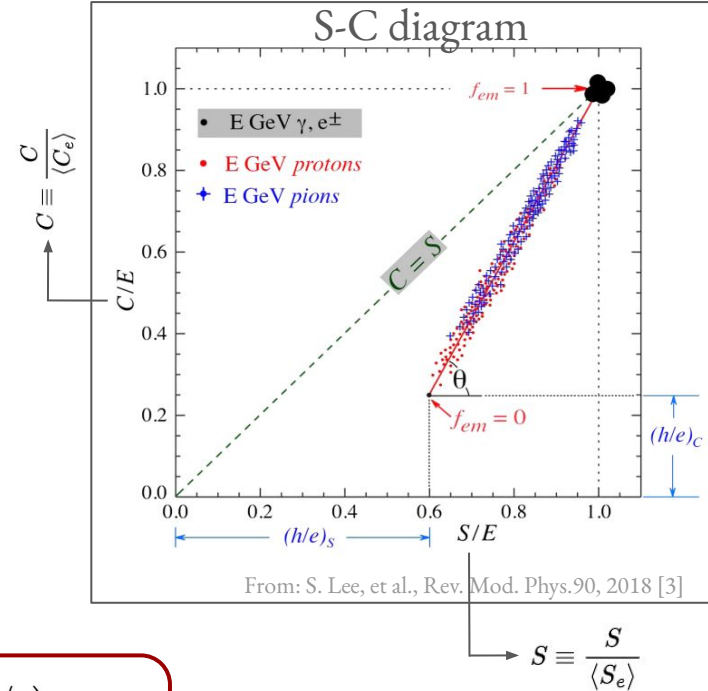
- ➔ Energy detection technique that improves measurement accuracy by using **two types of readings** to correct complex hadron interactions in calorimeters:
  - Scintillation (**S**) signals
  - Cherenkov (**C**) signals
- Both signals can be calibrated with electrons of known E energy.
- The dual-readout method works thanks to the fact that  $(\mathbf{e}/\mathbf{h})_S \neq (\mathbf{e}/\mathbf{h})_C$ . The larger the difference between both values, the better the e.m. shower fraction  $f_{em}$  can be extrapolated.

$$\begin{cases} S = E \left[ f_{em} + \frac{1}{(e/h)_S} (1 - f_{em}) \right] \\ C = E \left[ f_{em} + \frac{1}{(e/h)_C} (1 - f_{em}) \right] \end{cases}$$



$$f_{em} = \frac{(h/e)_C - (C/S)(h/e)_S}{(C/S) [1 - (h/e)_S] - [1 - (h/e)_C]}$$

- ⇒ Use of 2 photodetectors to extract signals and obtain the (C/S) ratio.
- ⇒ Objective : extract the  $f_{em}$  from the pulse shape using 1 photodetector



# Outlines

1. Calorimeter background
2. Dual-readout calorimetry
3. **Simulation**
4. Pulse shape discrimination
5. Reconstruction energy
6. Conclusion & Ongoing work

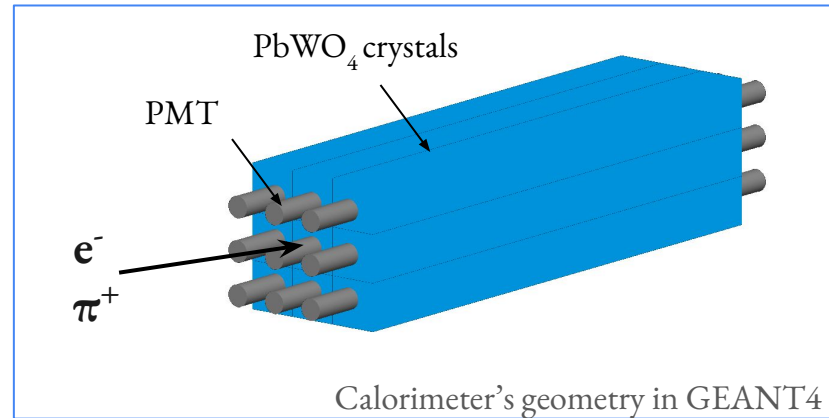
### 3. Simulation

- **Homogeneous** calorimeter made of 3x3  $\text{PbWO}_4$  crystals of dimensions:  
 $2.2 \times 2.2 \times 25 \text{ cm}^3$  (~ CMS ECAL).
- $\pi^+$  and  $e^-$  are shot in the center crystal of the calorimeter.

- $f_{em}$  implementation:

$$f_{em,sim} = \frac{E_{em}}{E_{tot}}$$

- Data extracted from the simulation:
  - Numbers of **C** and **S** photons detected at the PMT
  - **Pulse** shape at the PMT
  - $f_{em,sim}$

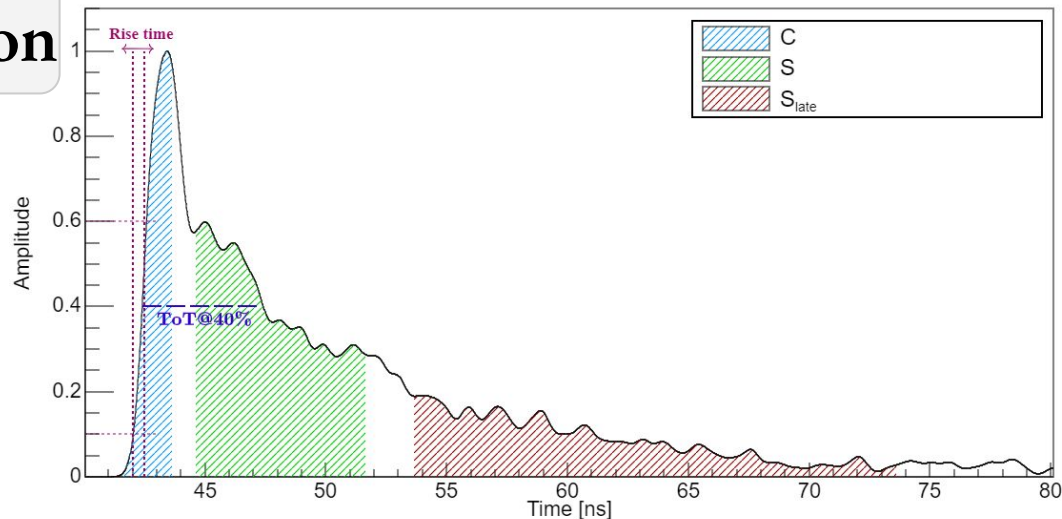
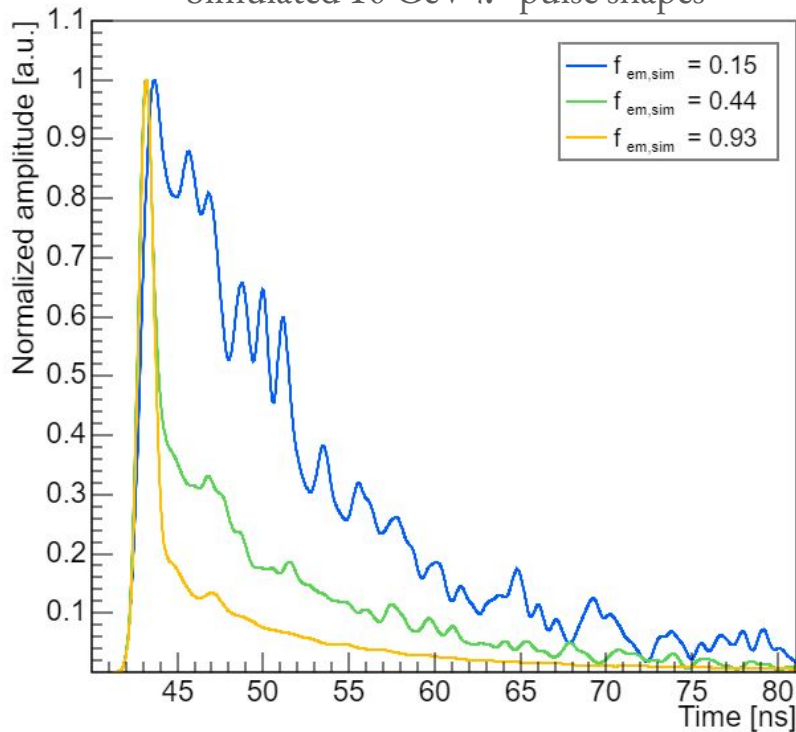


# Outlines

1. Calorimeter background
2. Dual-readout calorimetry
3. Simulation
- 4. Pulse shape discrimination**
5. Reconstruction energy
6. Conclusion & Ongoing work

## 4. Pulse shape discrimination

Simulated 10 GeV  $\pi^+$  pulse shapes

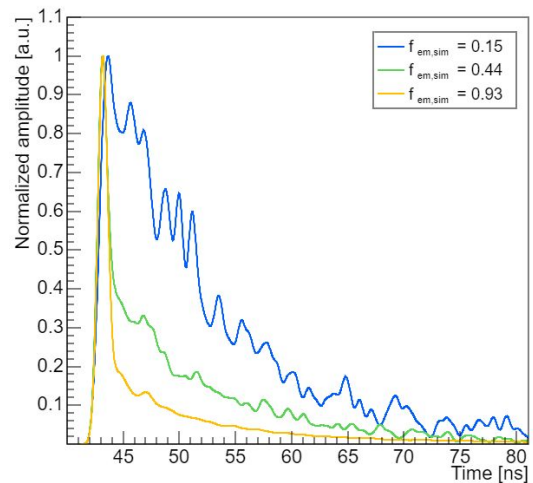
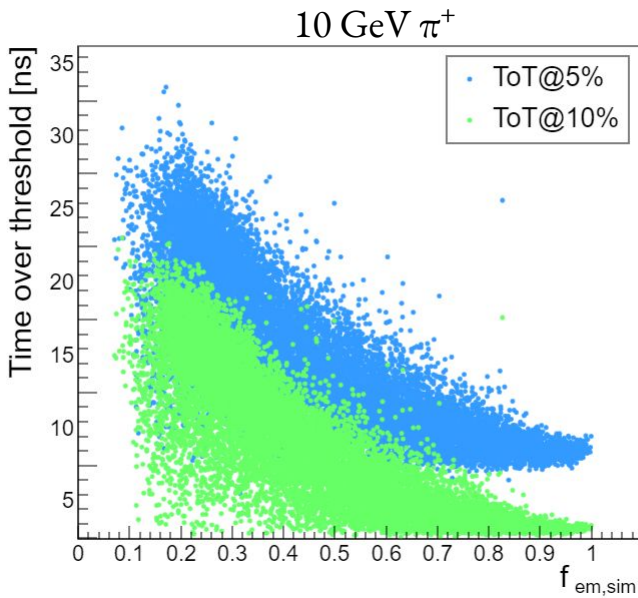
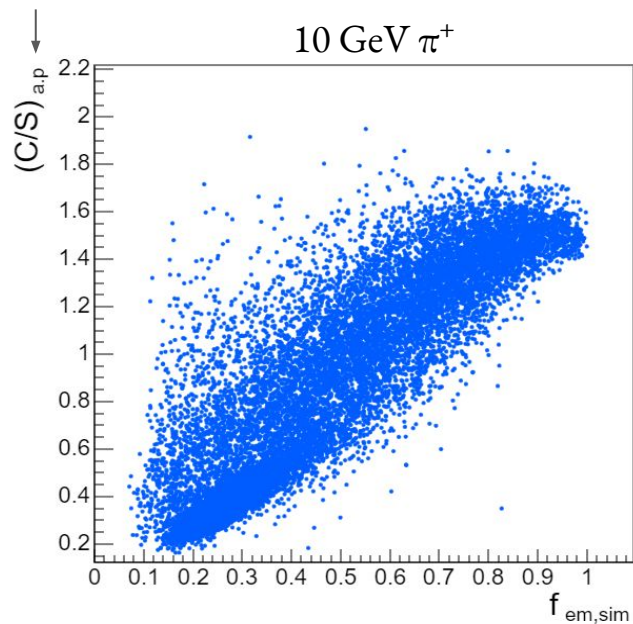


### Features :

- **C, S, S<sub>late</sub>** areas
  - **rise time** (= time to go from 10% to 60% of the pulse amplitude)
  - time over threshold (**ToT**) at different percentages
- Possibility of combining features with machine learning (ML) using a boost decision tree.

## ☐ Some features extracted from the pulse

Ratio of C and S areas of the pulse (a.p.)



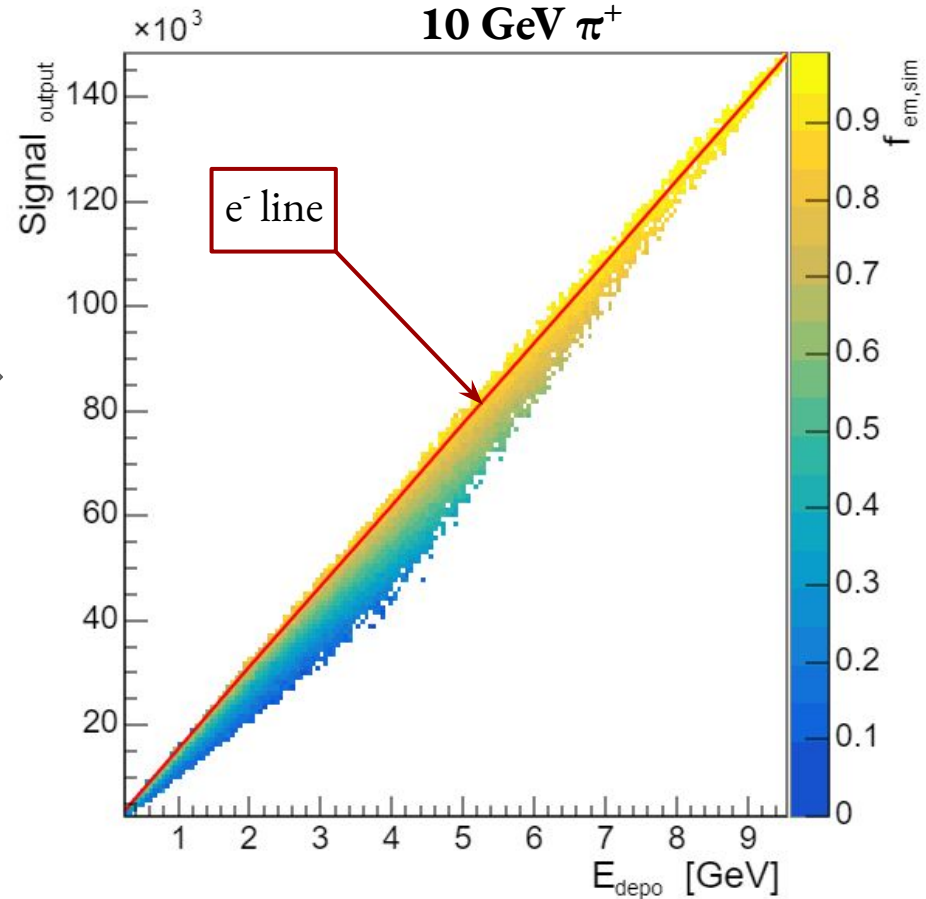


# Outlines

1. Calorimeter background
2. Dual-readout calorimetry
3. Simulation
4. Pulse shape discrimination
- 5. Energy reconstruction**
6. Conclusion & Ongoing work

## 4. Energy reconstruction

$$\left( \frac{\text{Signal}_{\text{output}}}{E_{\text{depo}}} \right)_{h.} = e f_{em} + h (1 - f_{em})$$

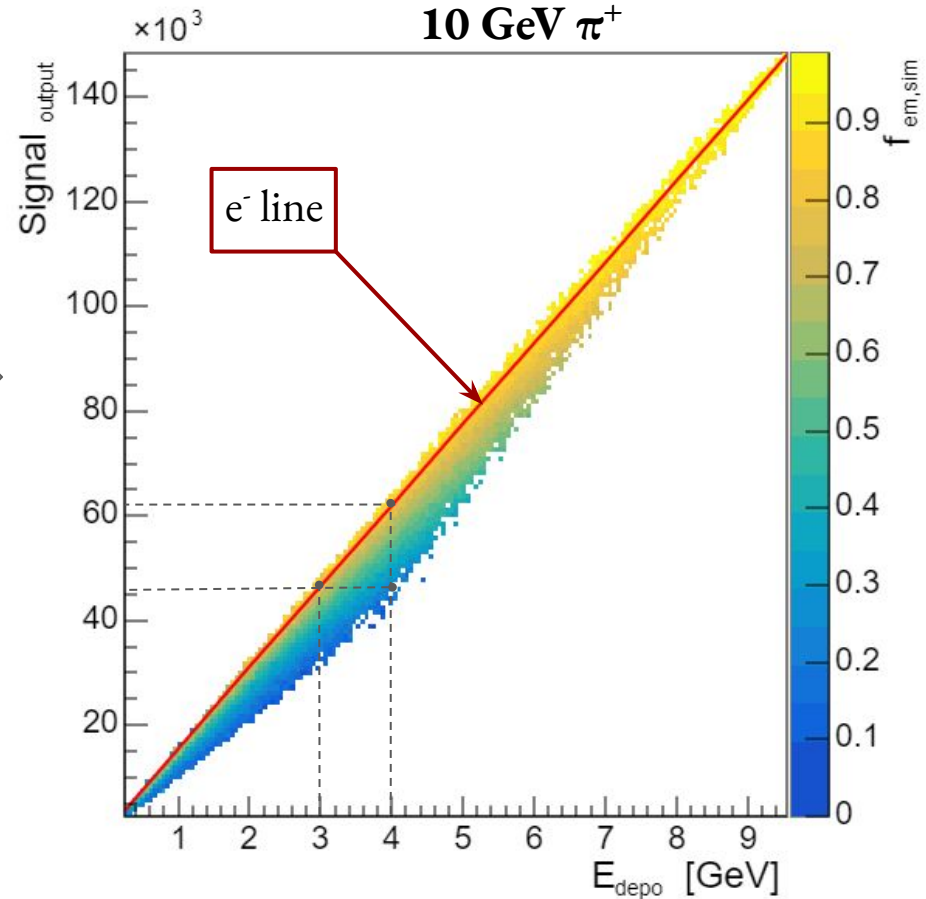


## 4. Energy reconstruction

$$\left( \frac{\text{Signal}_{\text{output}}}{E_{\text{depo}}} \right)_{h.} = e f_{em} + h (1 - f_{em})$$



→ Underestimate the real energy deposited by  $\pi^+$



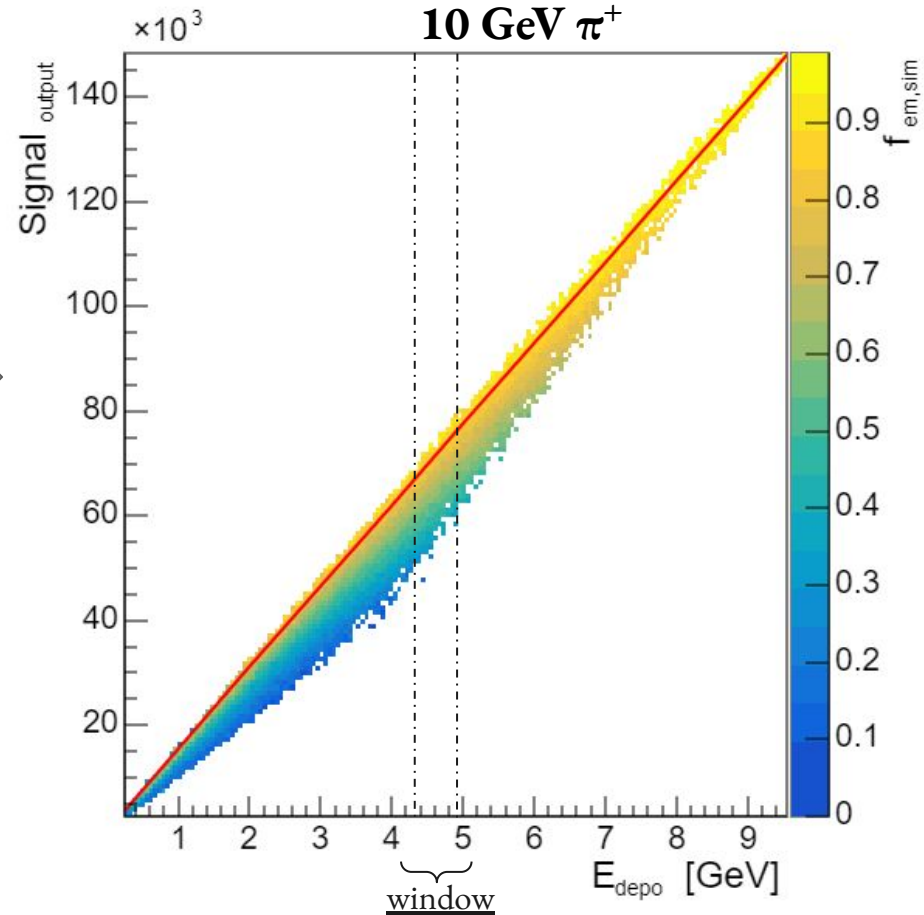
## 4. Energy reconstruction

$$\left( \frac{\text{Signal}_{\text{output}}}{E_{\text{depo}}} \right)_h = e f_{em} + h (1 - f_{em})$$

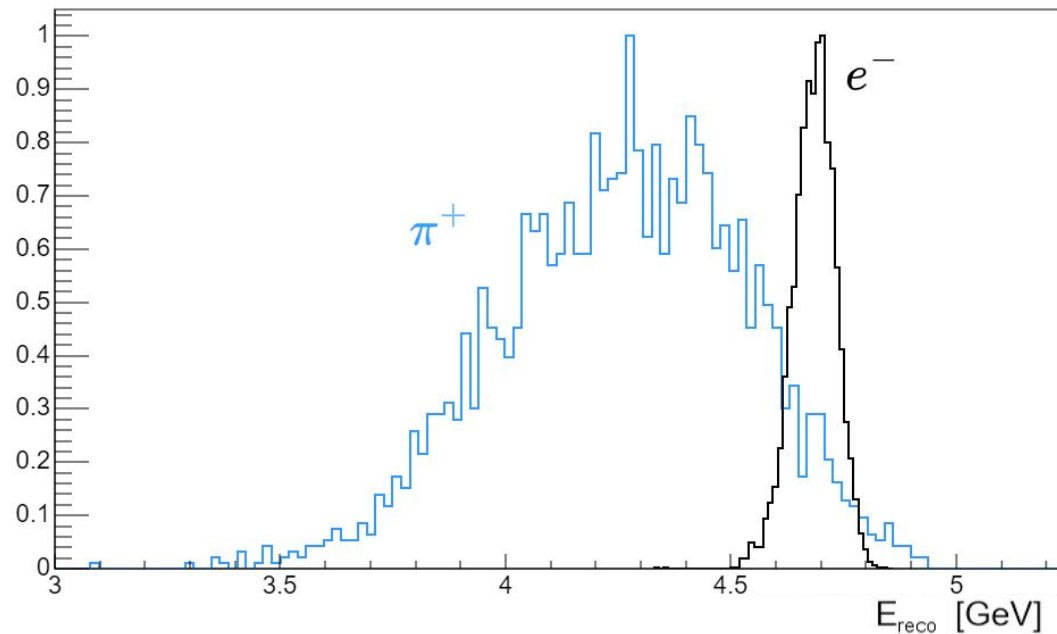
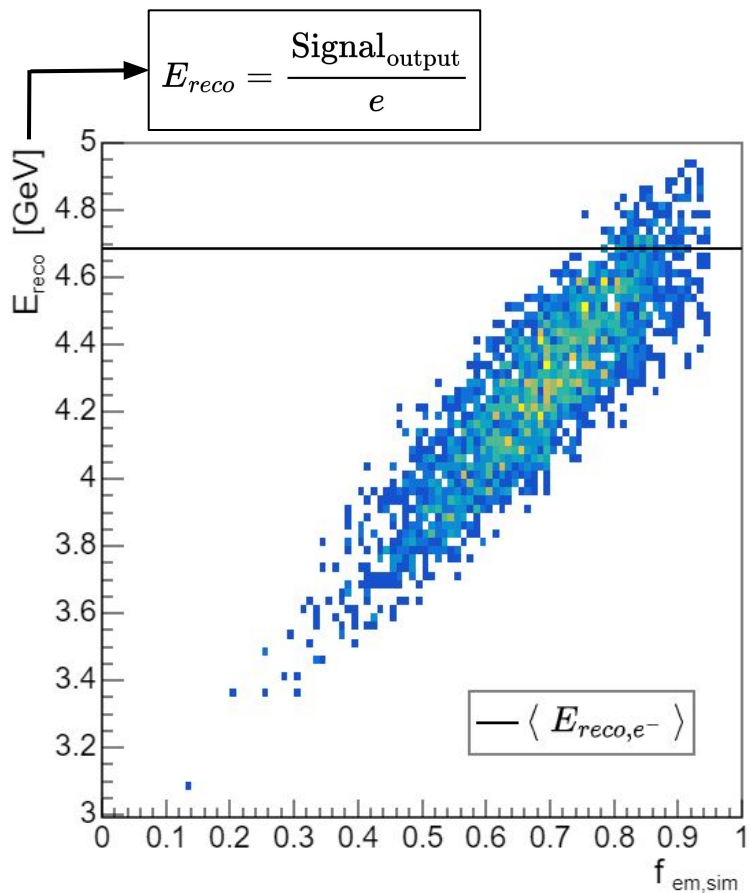


→ Look at events that deposited energy in a window :

$$4.37 \text{ GeV} \leq E_{\text{depo}} \leq 4.81 \text{ GeV}$$



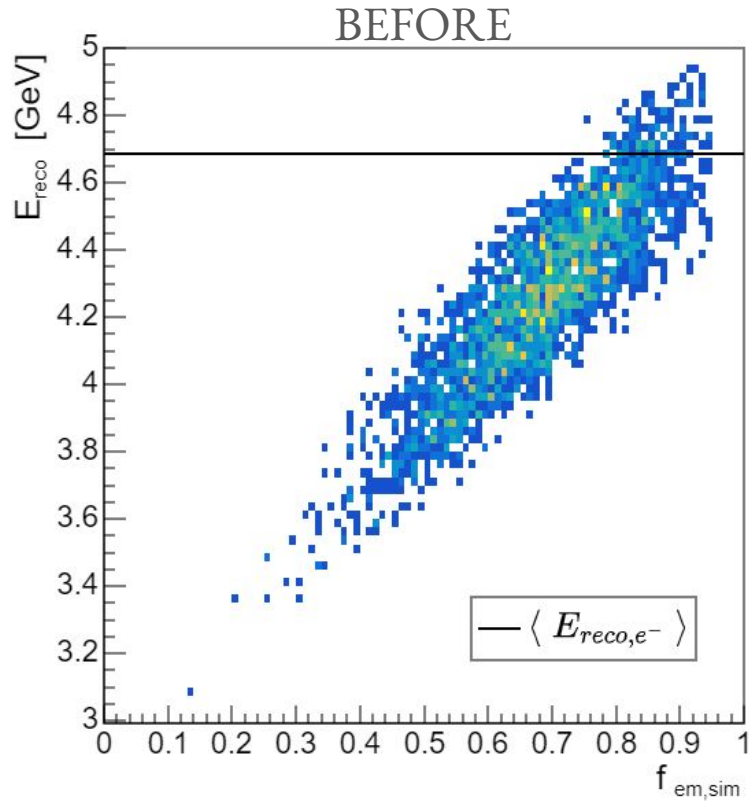
□ **Before calibration (b. calib.)**



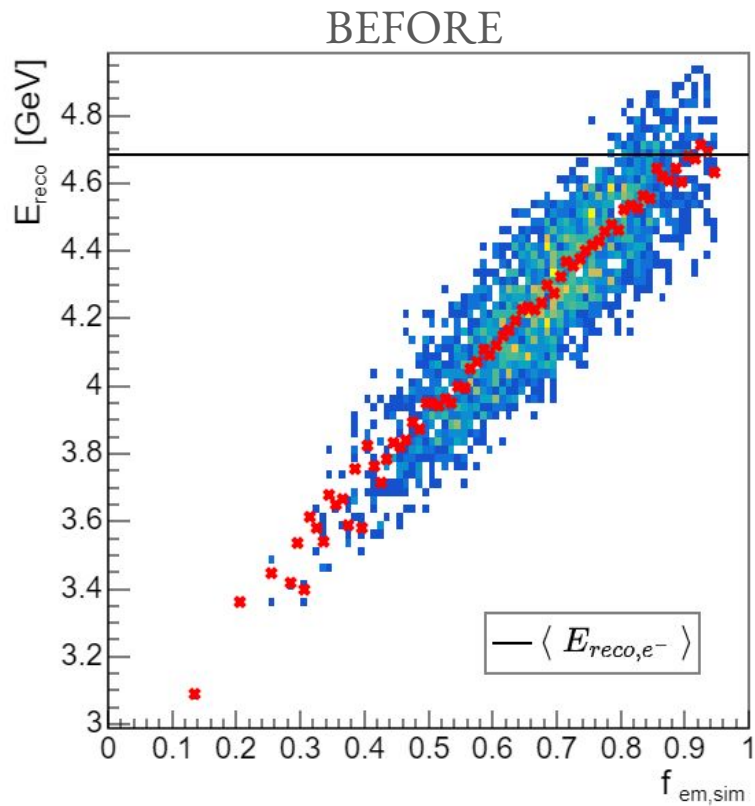
Energy resolution for  $e^-$ :  $\frac{\sigma_{e^-}}{\langle E_{e^-} \rangle} = (1.03 \pm 0.01)\%$

Energy resolution for  $\pi^+$ :  $\frac{\sigma_{\pi^+}}{\langle E_{\pi^+} \rangle} = (6.38 \pm 0.09)\%$

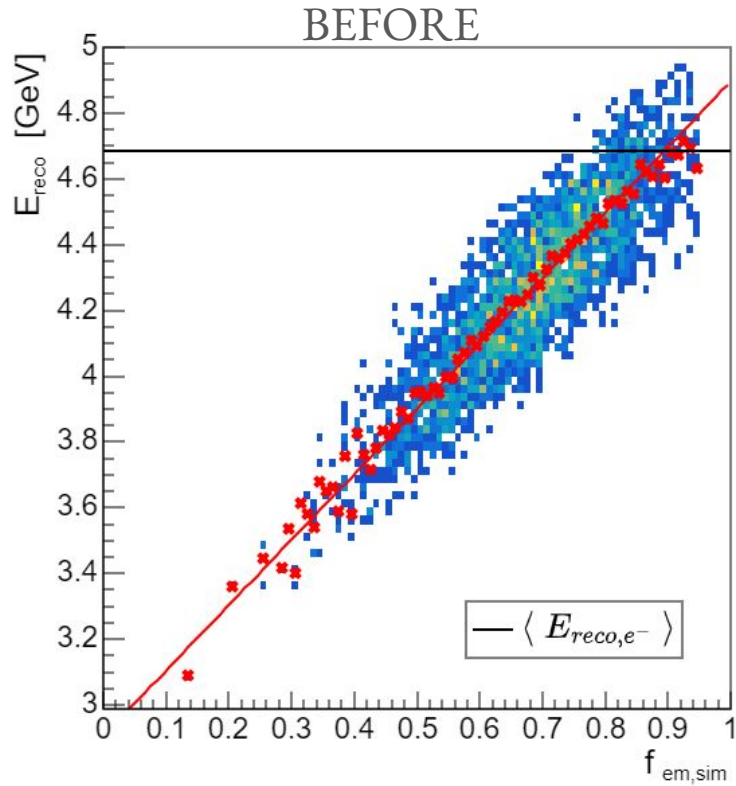
## Calibration method



## Calibration method

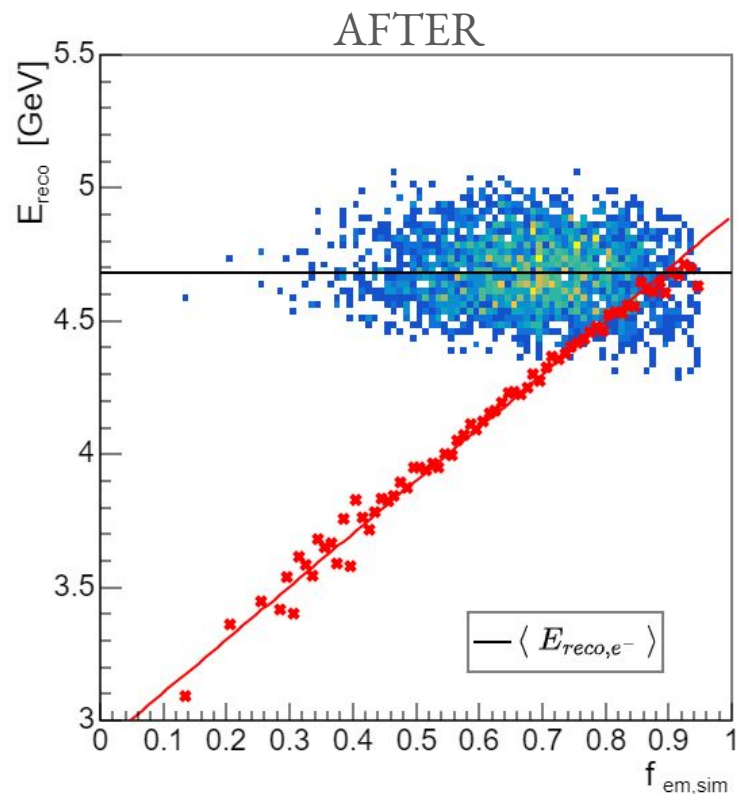
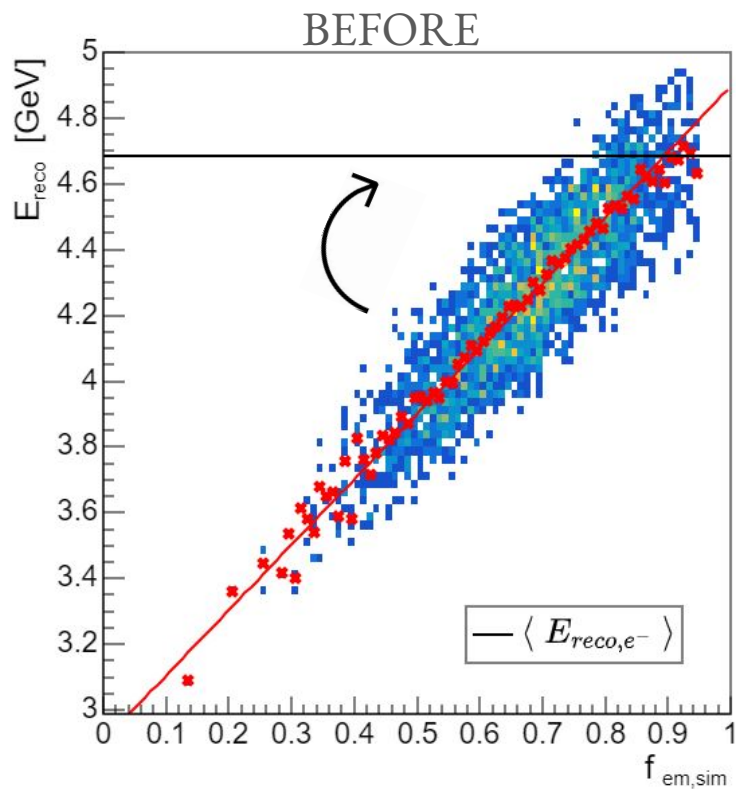


## Calibration method





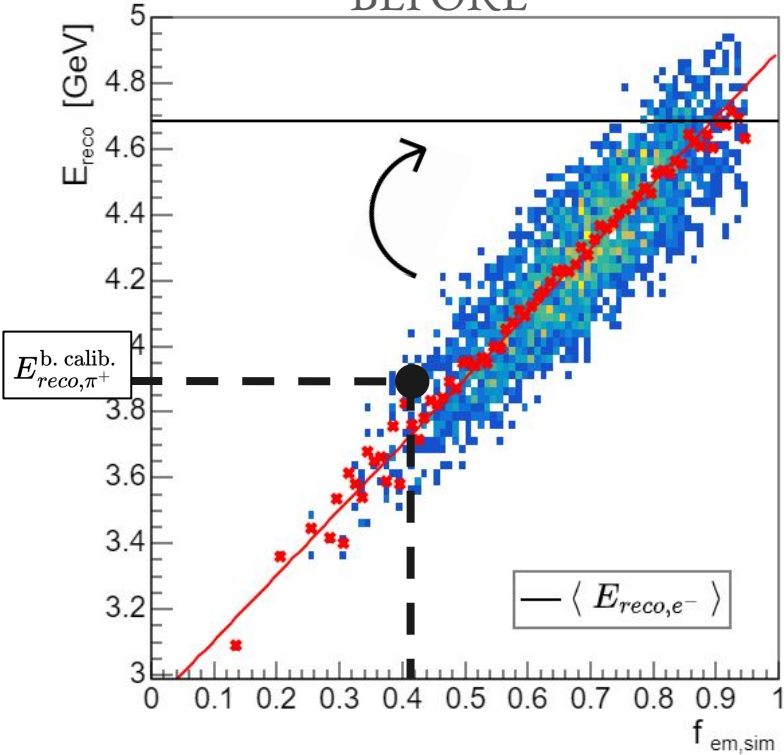
## Calibration method



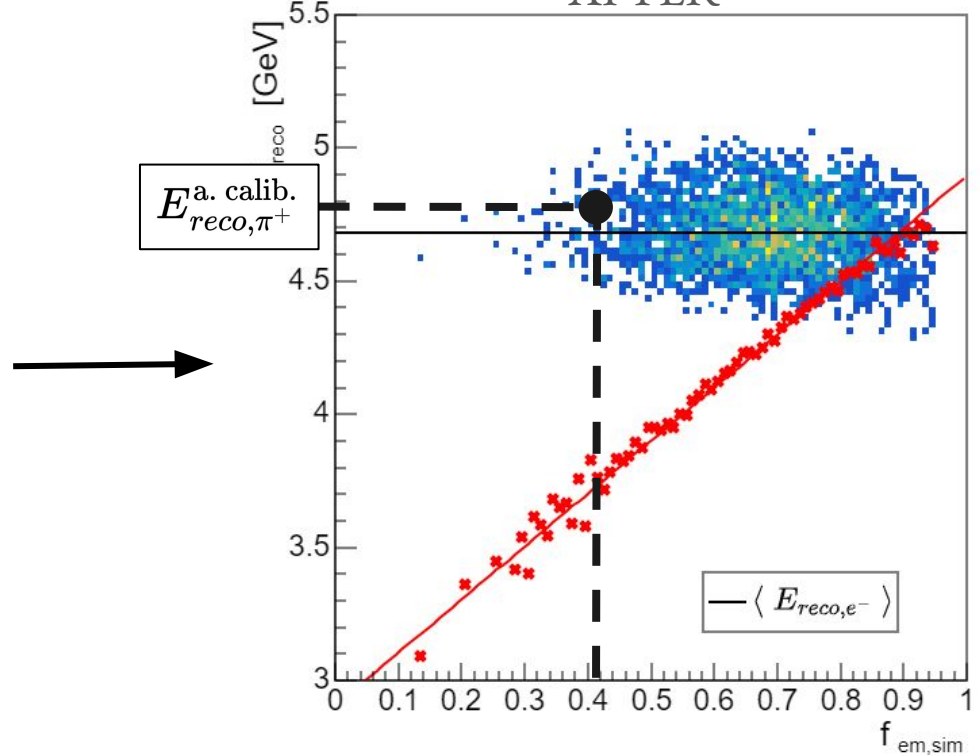
# Calibration method

$$E_{reco,\pi^+}^{a. calib.}(f_{em}) = E_{reco,\pi^+}^{b. calib.} + \langle E_{reco,e^-} \rangle - [af_{em,sim} + b]$$

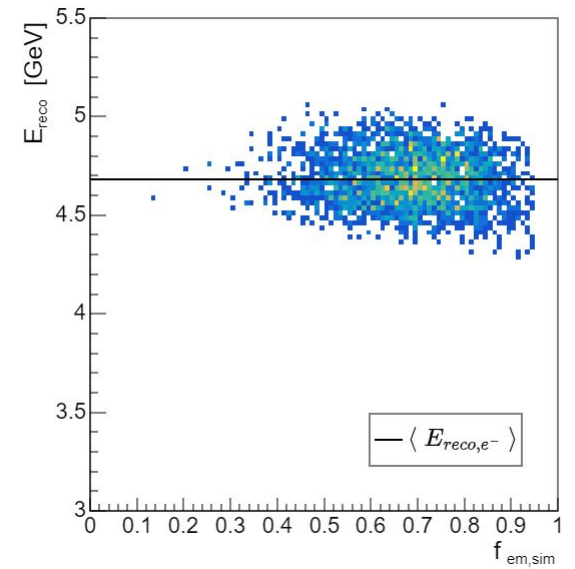
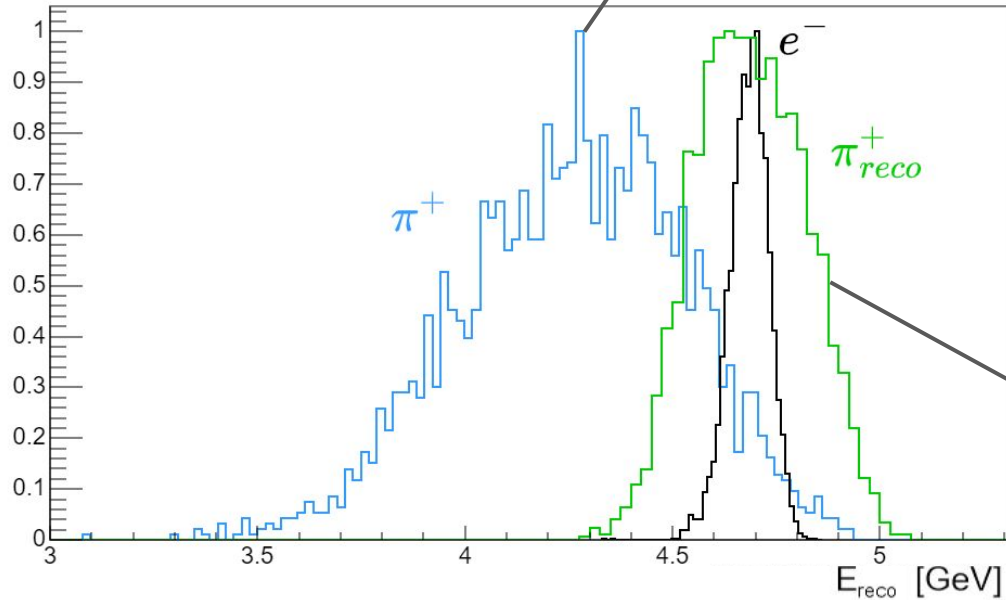
BEFORE



AFTER



After calibration

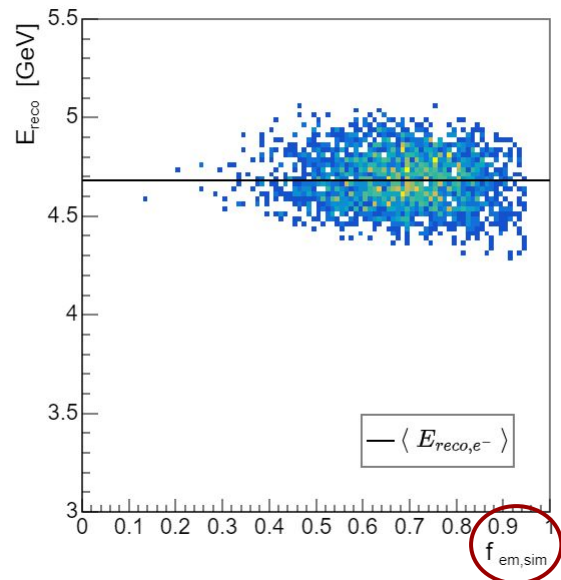
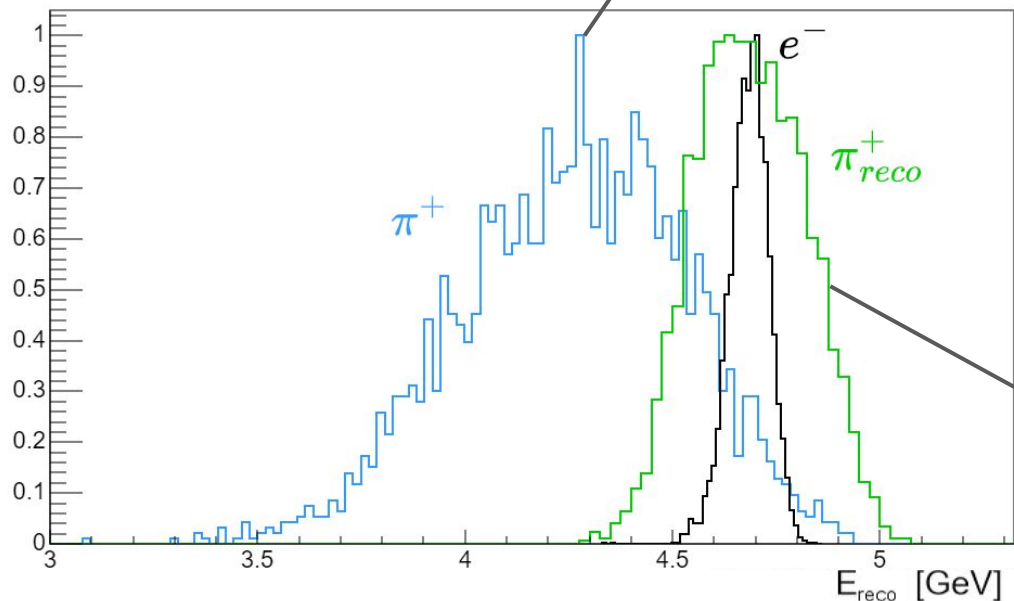


$$\left( \frac{\sigma_{reco,\pi^+}}{\langle E_{reco,\pi^+} \rangle} \right)_{f_{em,sim}} = (2.79 \pm 0.04)\%$$

Tables with the results obtained from the different **features** used to do the calibration:

Features	$(C/S)_{\text{detected photons}}$	$(C/S)_{\text{area pulse}}$	ToT@5%	$f_{em,ML}$
$\frac{\sigma_{reco,\pi^+}}{\langle E_{reco,\pi^+} \rangle}$	$(3.38 \pm 0.05)\%$	$(3.62 \pm 0.05)\%$	$(3.69 \pm 0.05)\%$	$(3.55 \pm 0.05)\%$ <i>Preliminary</i>

After calibration



$$\left( \frac{\sigma_{reco,\pi^+}}{\langle E_{reco,\pi^+} \rangle} \right)_{f_{em,sim}} = (2.79 \pm 0.04)\%$$

Tables with the results obtained from the different **features** used to do the calibration:

Features	$(C/S)_{\text{detected photons}}$	$(C/S)_{\text{area pulse}}$	ToT@5%	$f_{em,ML}$
$\frac{\sigma_{reco,\pi^+}}{\langle E_{reco,\pi^+} \rangle}$	$(3.38 \pm 0.05)\%$	$(3.62 \pm 0.05)\%$	$(3.69 \pm 0.05)\%$	$(3.55 \pm 0.05)\%$ <i>Preliminary</i>



# Outlines

1. Calorimeter background
2. Dual-readout calorimetry
3. Simulation
4. Pulse shape discrimination
5. Reconstruction energy
- 6. Conclusion & Ongoing work**

## 5. Conclusion & Ongoing work

- Proportionality shown between the **features extracted from the pulse shape** with the  $f_{em}$ .
- Maximizing the information from the ECAL by extracting proportional features of the  $f_{em}$  information from the **pulse shape** at the photodetector event by event.
  - ↳ Information extracted from **only 1 photodetector** instead of using 2 as done normally.
- Possibility of combining features to estimate the  $f_{em}$  using a machine learning algorithm :
  - ↳ Reconstruction of the energy with a better resolution.

### Next steps:

- ❖ Improvement on the ML algorithm.
- ❖ Applying the techniques developed to a realistic configuration, as in a testbeam or a full detectors.
- ❖ Including a HCAL in simulation to allow full containment of the shower and evaluate the influence of the ECAL with dual readout capability on the performance, the results will be evaluated with experimental measurements in testbeam. From: Lucchini M.T., et al., JINST 15 P11005, 2020 [4]

# Thank you for your attention !

This work was supported by the Horizon Europe ERA Widening Project no. 101078960 “TWISMA”.

# References

- [1] - Roldan, Pablo & Lecoq, Paul, Quality control and preparation of the PWO crystals for the electromagnetic calorimeter of CMS. (2011)
- [2] - Auguste Besson, extract of chapter 6 “High Energy” of “Particle interaction with matter In nuclear and particle physics” lecture, Strasbourg’s University. (2022)
- [3] - Sehwook Lee, Michele Livan, Richard Wigmans, Dual-readout calorimetry, Reviews of Modern Physics, volume 90 , <https://doi.org/10.1103/RevModPhys.90.025002>. (2018)
- [4] - Lucchini M.T., et al., New perspectives on segmented crystal calorimeters for future colliders, JINST 15 P11005. (2020)
- [5] - Particle Data Group. “Review of Particle Physics”. Progress of Theoretical and Experimental Physics (PTEP) 083C01. (2022)



# Backup slides

# □ Radiation-matter interaction

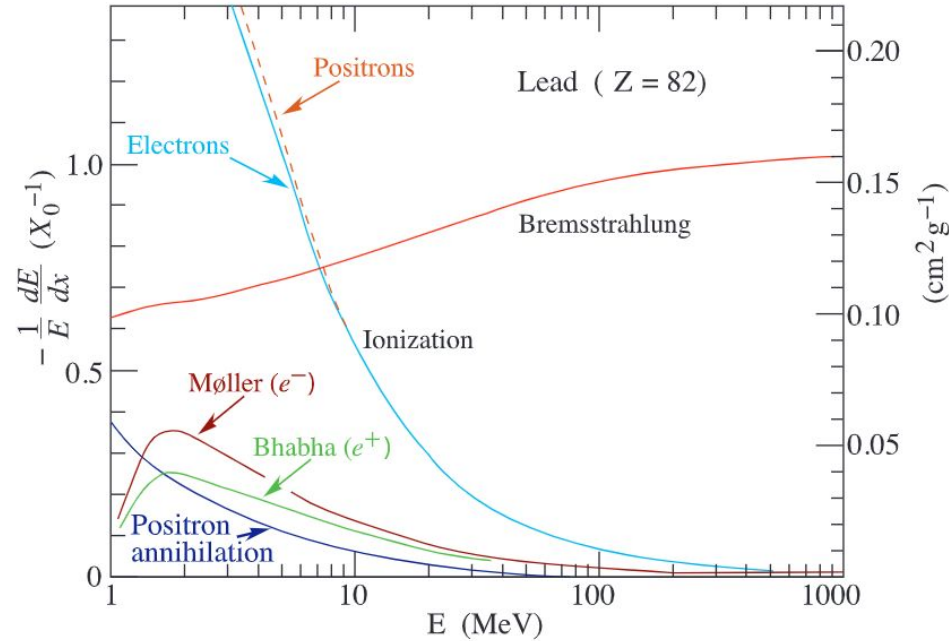


Figure 1 : Fractional energy loss per radiation length in lead as a function of electron or positron energy

From: Particle Data Group, PTEP 083C01, 2022 [5]

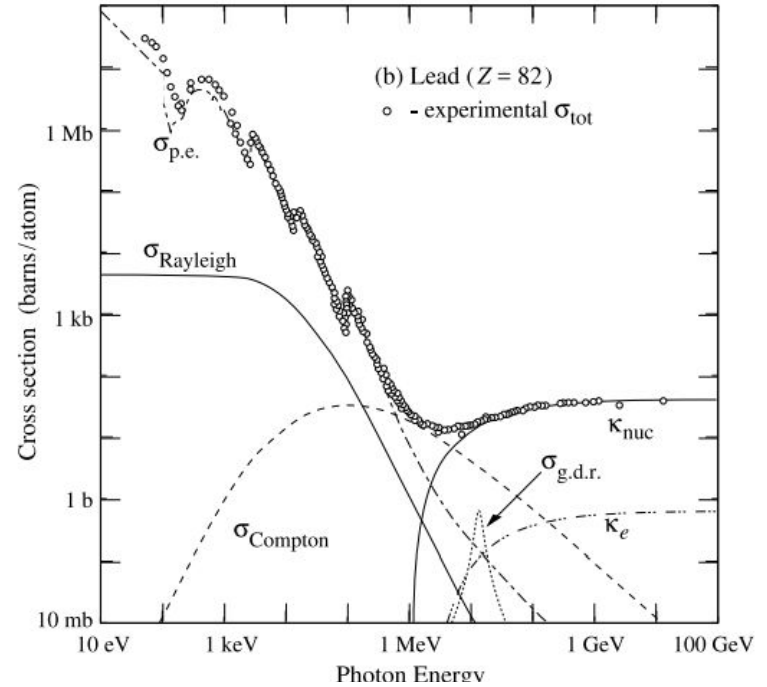
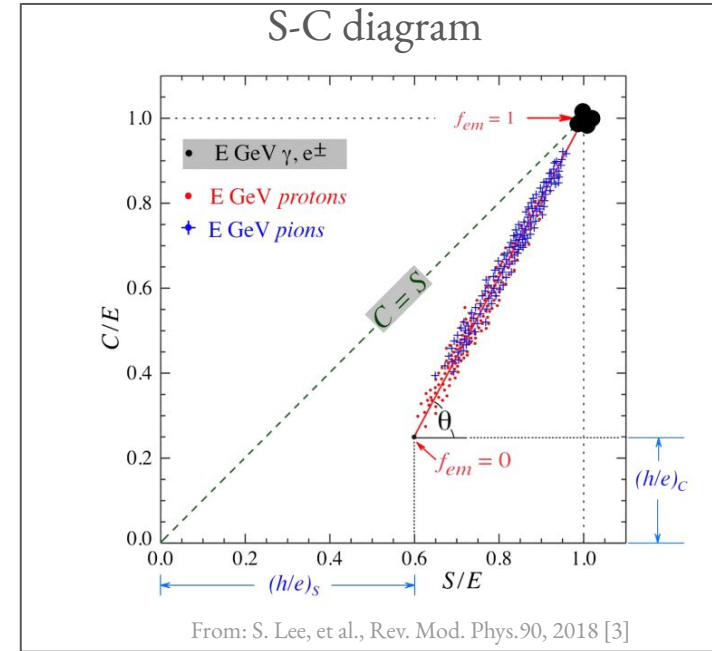
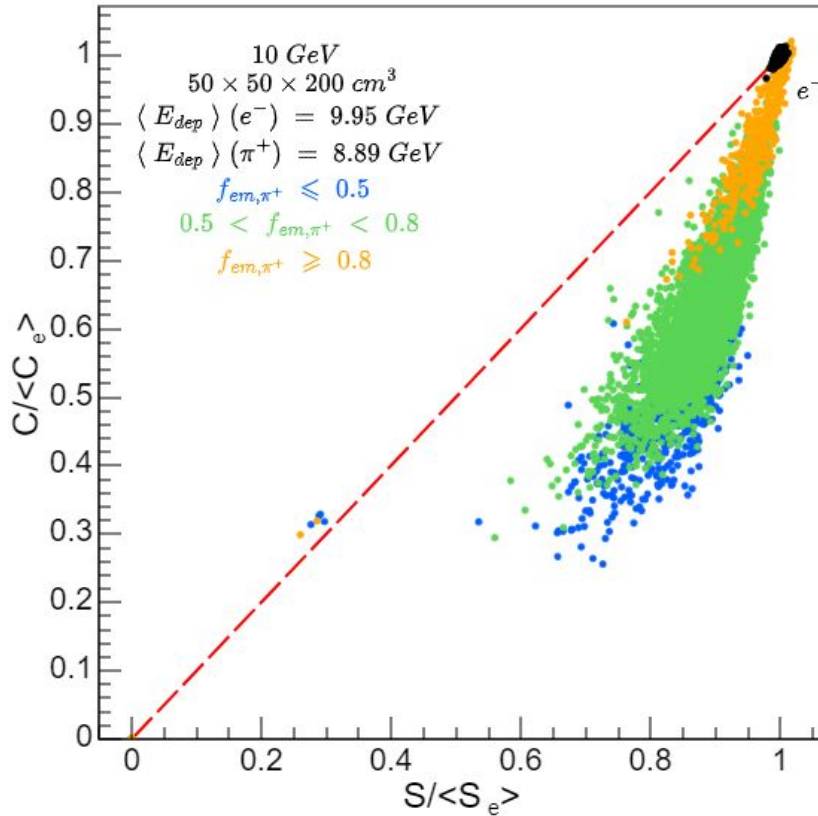


Figure 2 : Photon total cross sections as a function of energy in carbon and lead, showing the contributions of different processes

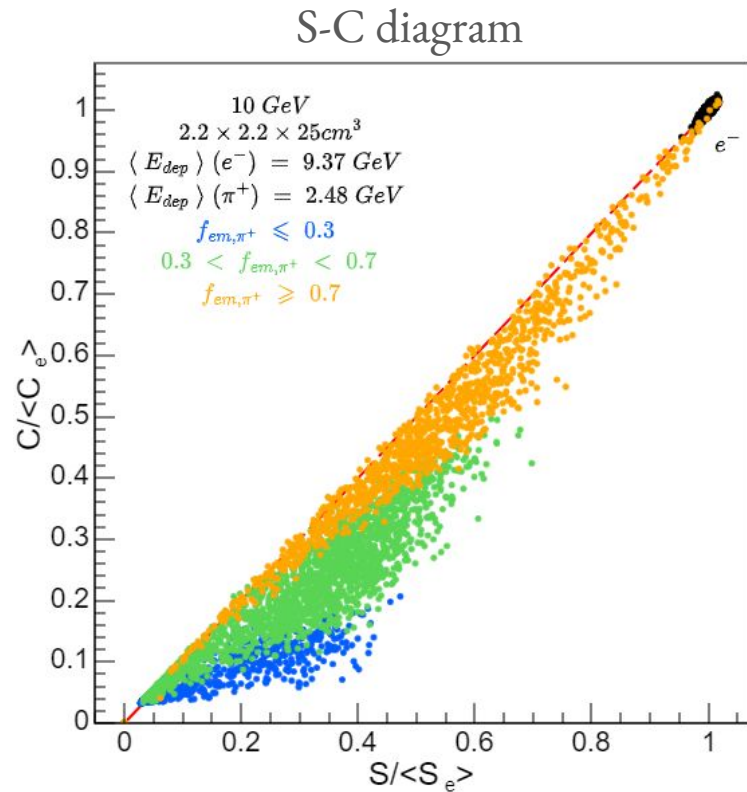
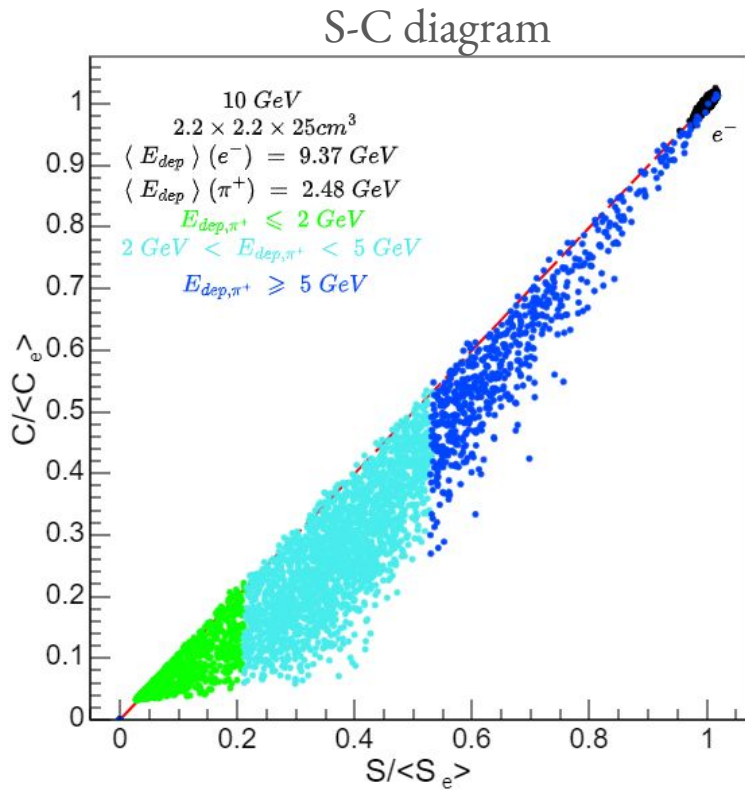
# HCAL dual-readout capabilities

S-C diagram



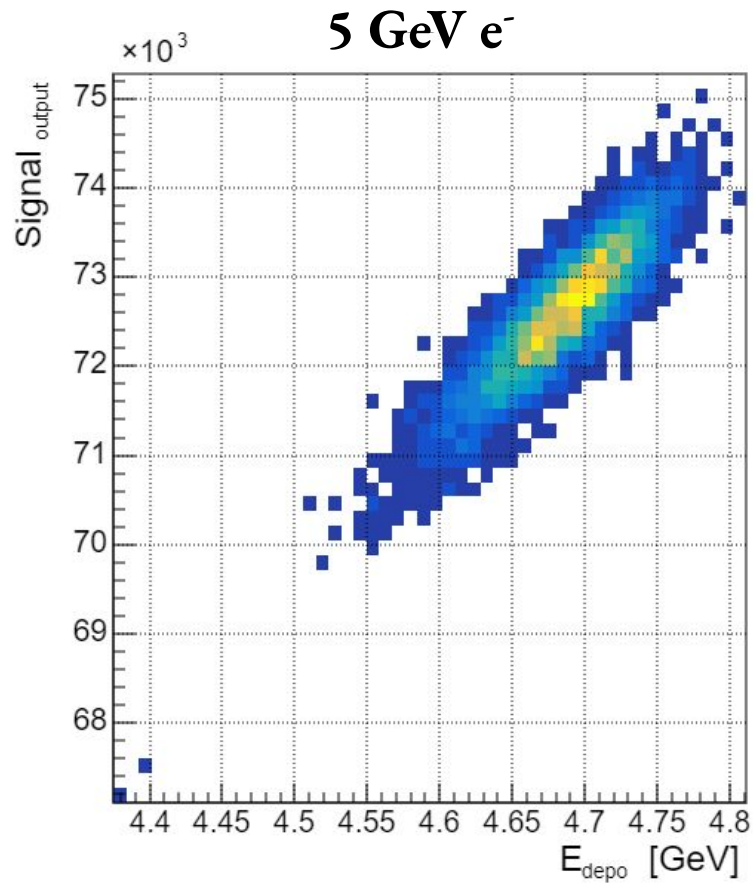
- $50 \times 50 \times 200 \text{ cm}^3$  ( $\sim$  HCAL) to test the dual-readout capabilities of the simulated calorimeter.

ECAL dual-readout capabilities

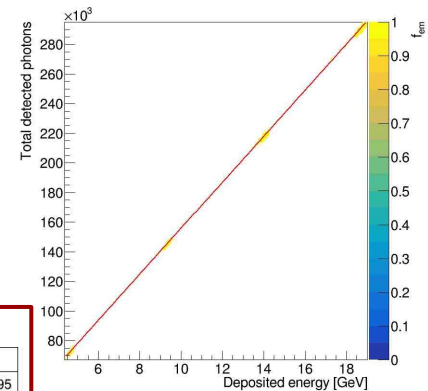
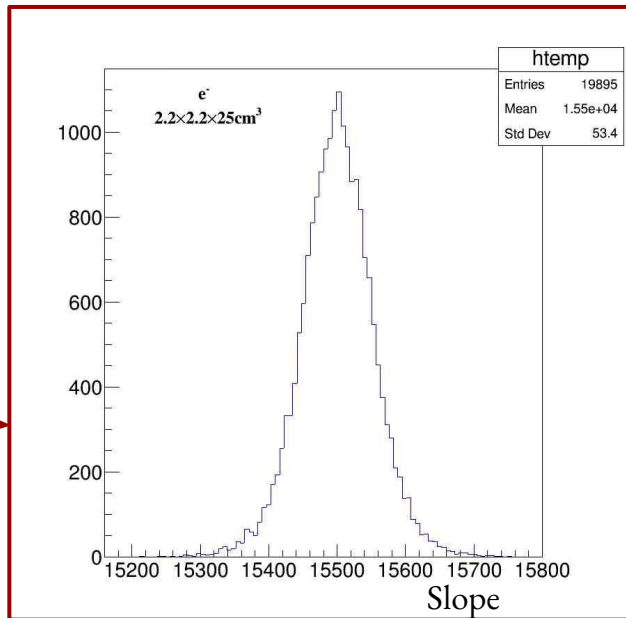
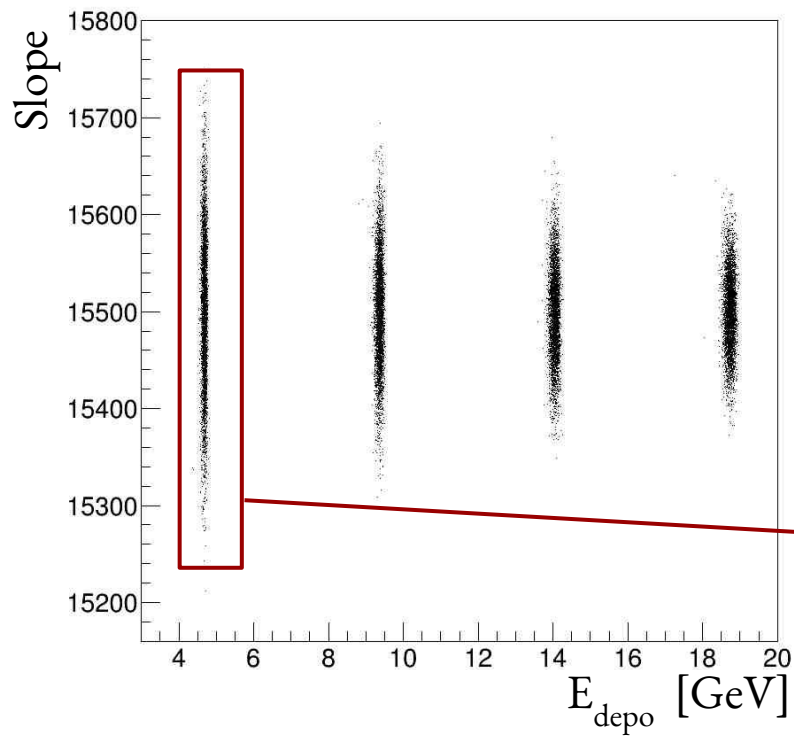


□  $E_{\text{reco}}$  of 5 GeV  $e^-$

$$4.37 \text{ GeV} \leq E_{\text{depo}} \leq 4.81 \text{ GeV}$$

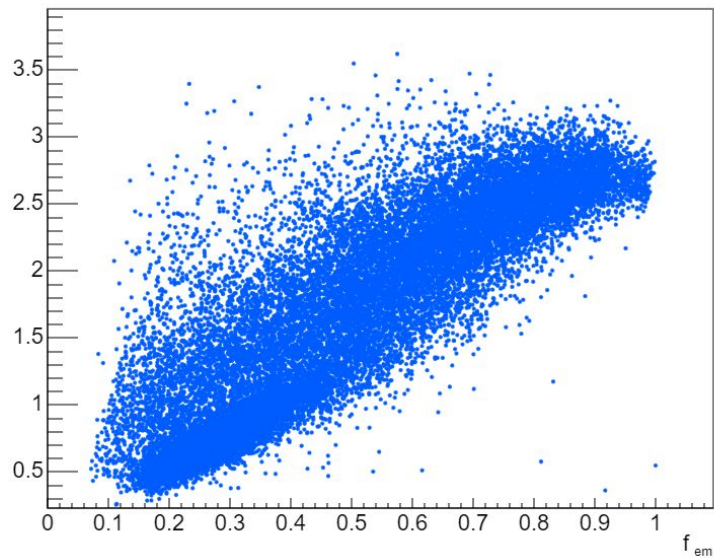


# □ Linearity for e.m. showers

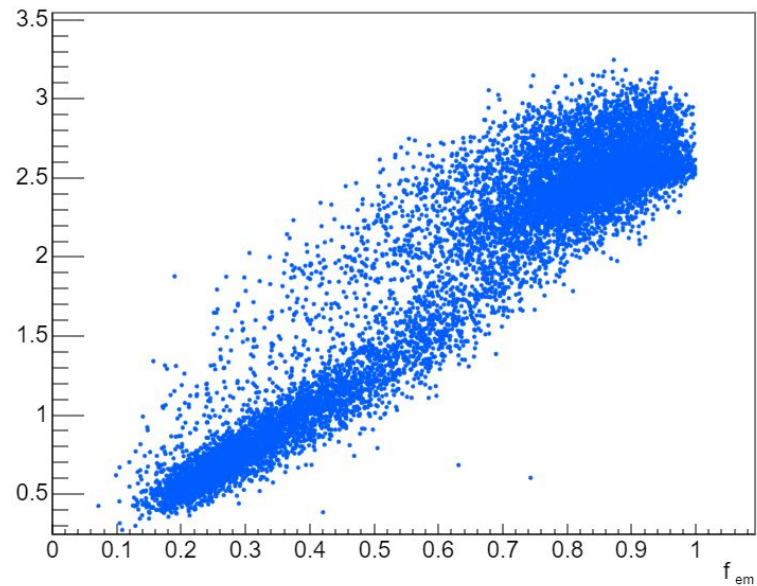


□ Features -  $(C/S)_{a.p.}$

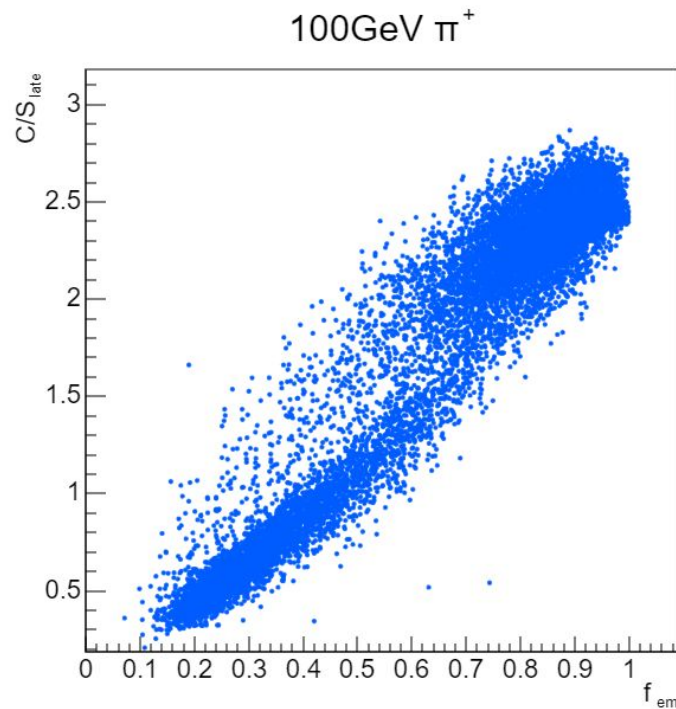
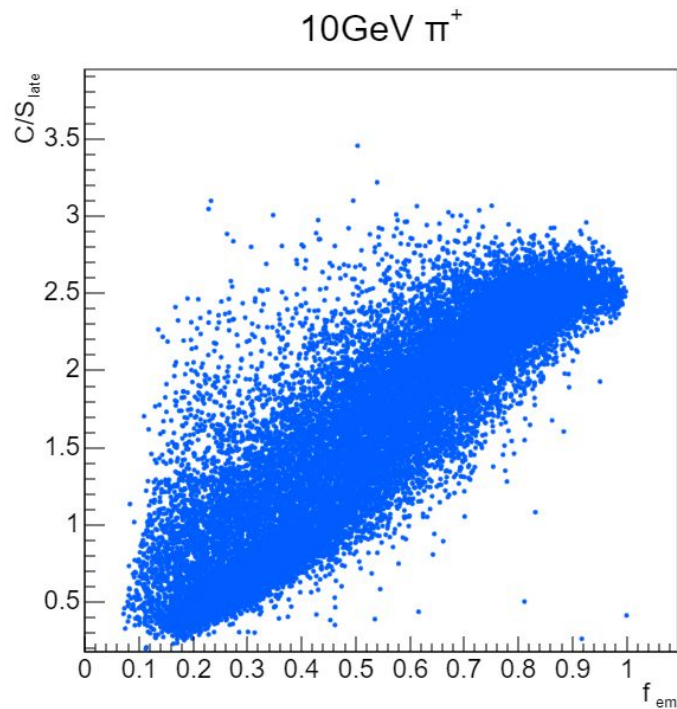
10GeV  $\pi^+$



100GeV  $\pi^+$

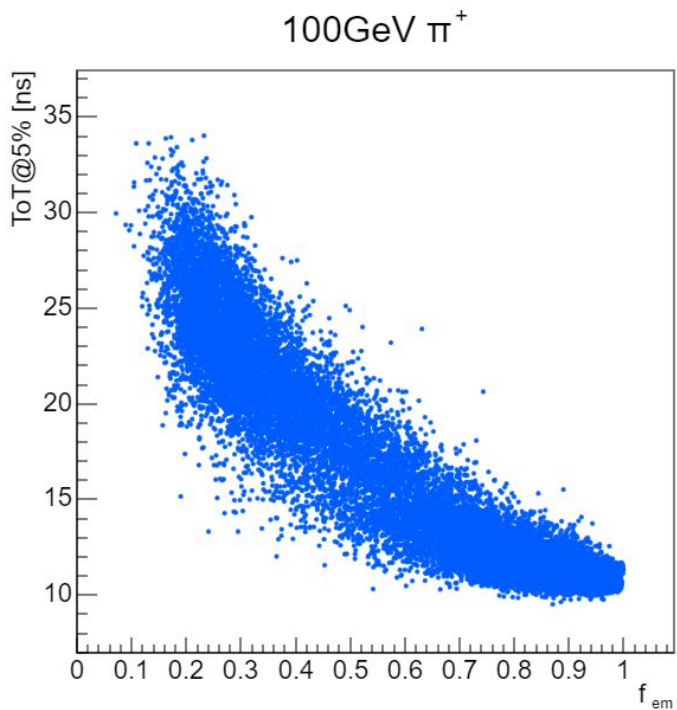
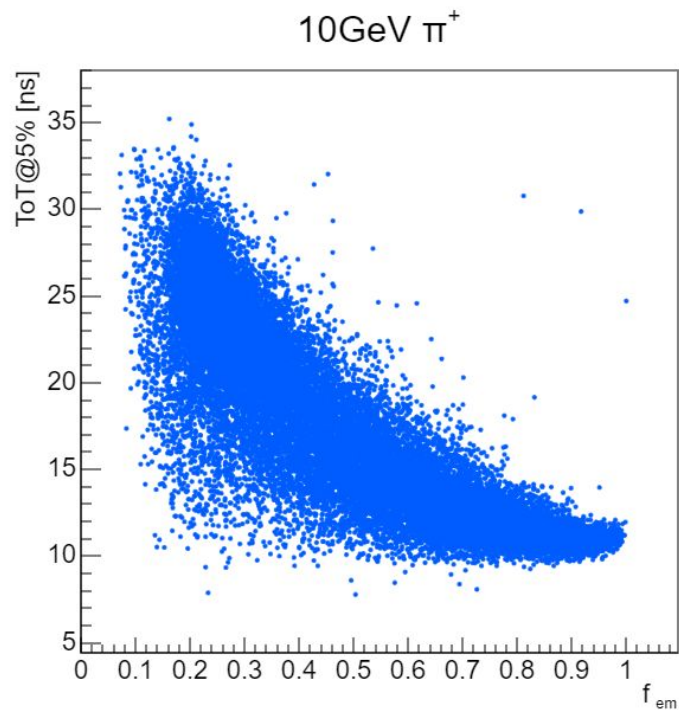


□ Features -  $(C/S_{\text{late}})_{\text{a.p.}}$

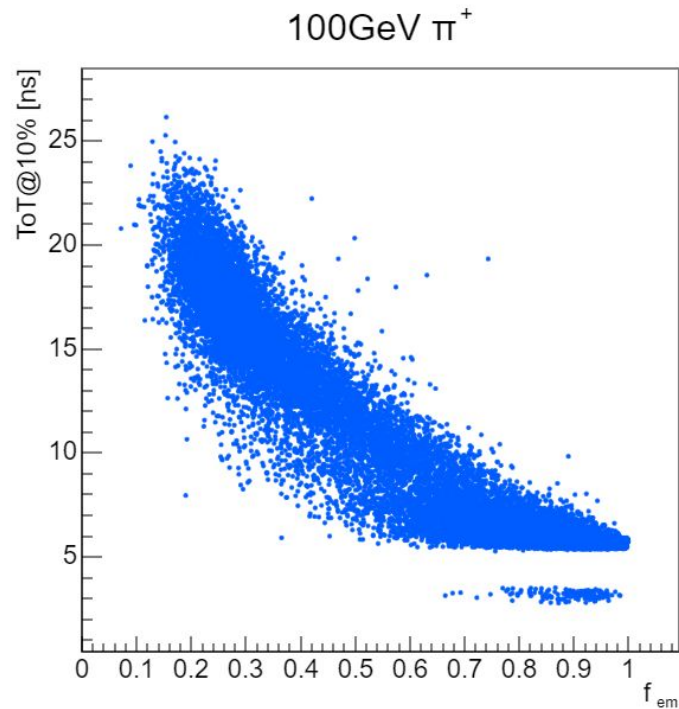
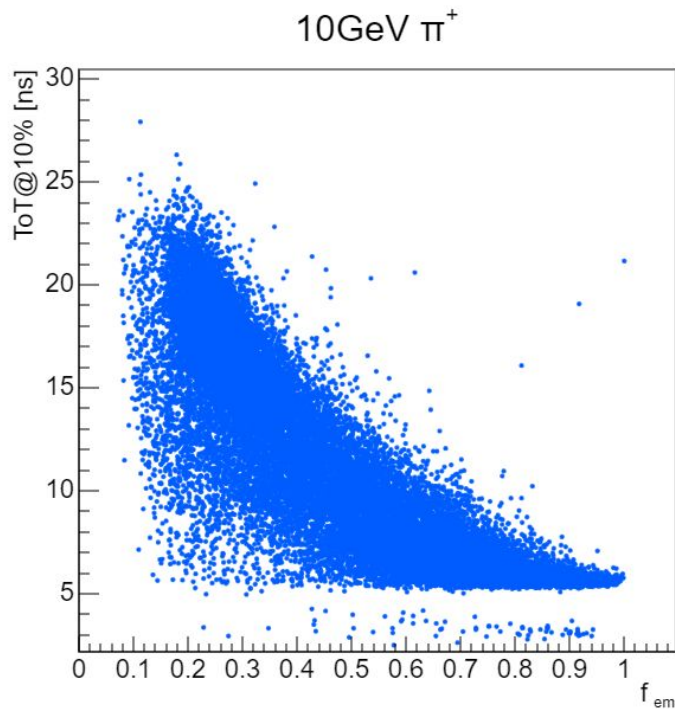




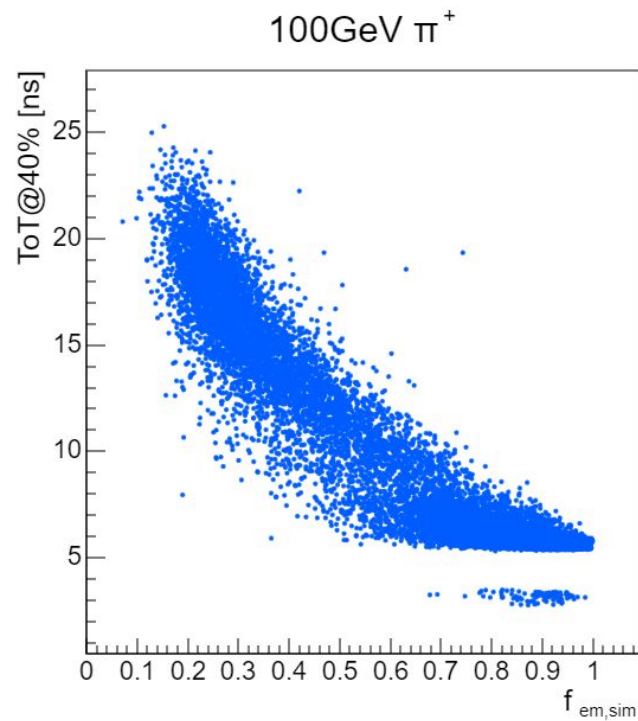
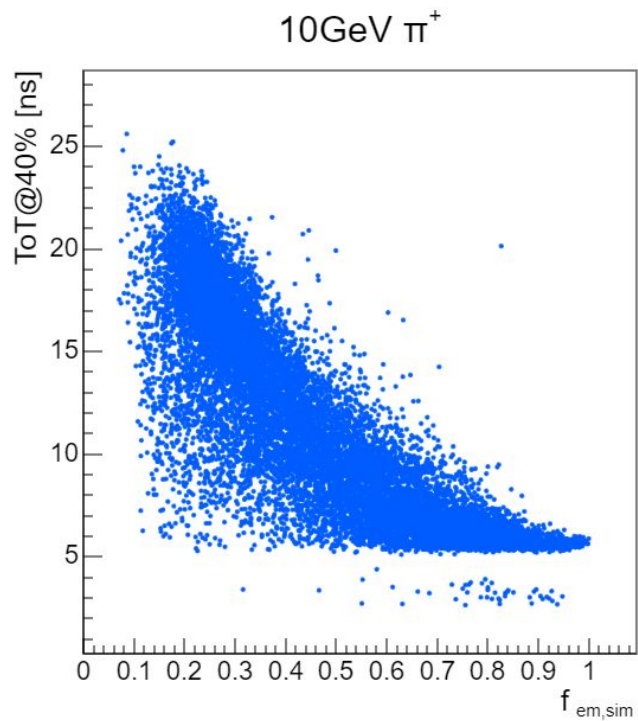
□ Features - ToT@5%



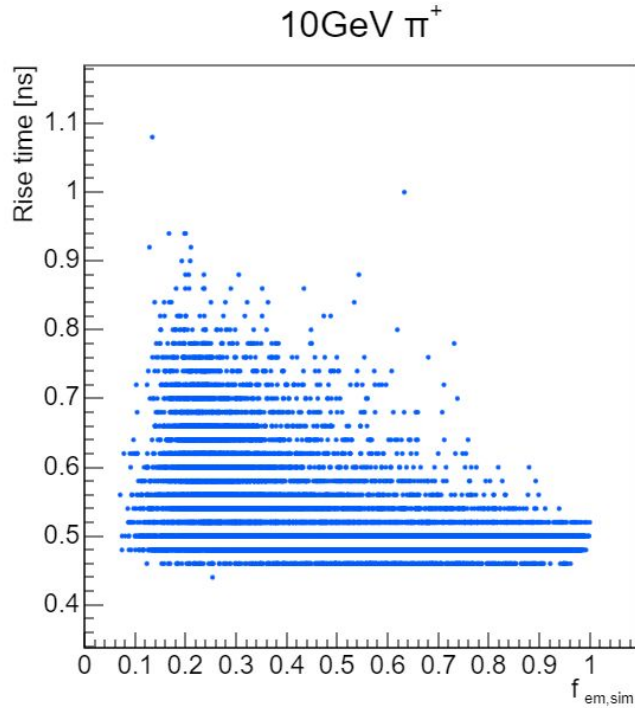
□ Features - ToT@10%



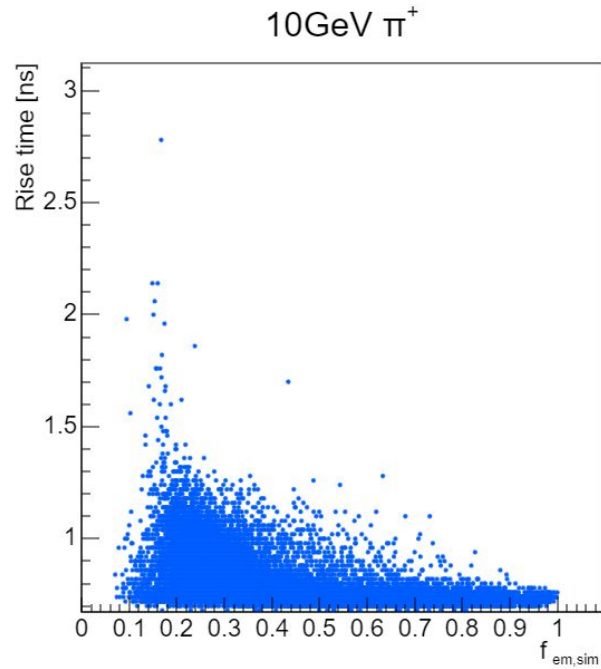
□ Features - ToT@40%



□ Features - Rise time



10% - 60%

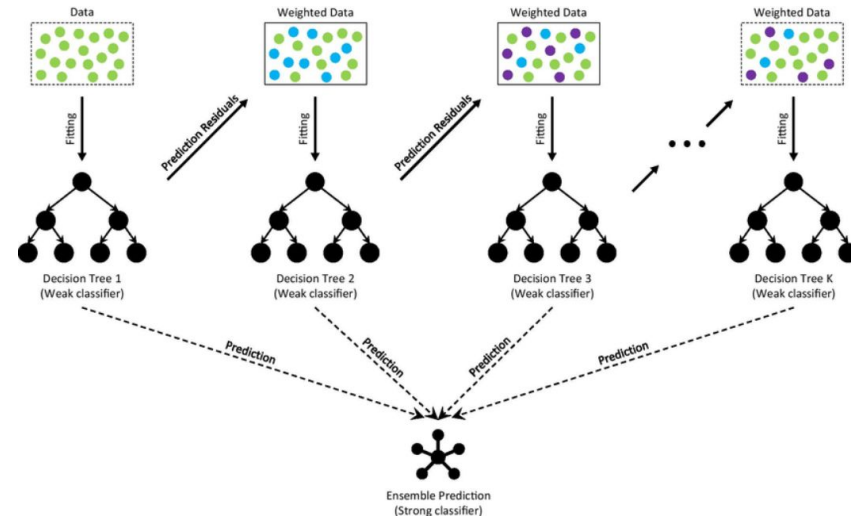


10% - 90%

# □ Gradient Boost Decision Tree

→ an ensemble technique that **combines the predictions of multiple decision trees to produce a more accurate and robust model.**

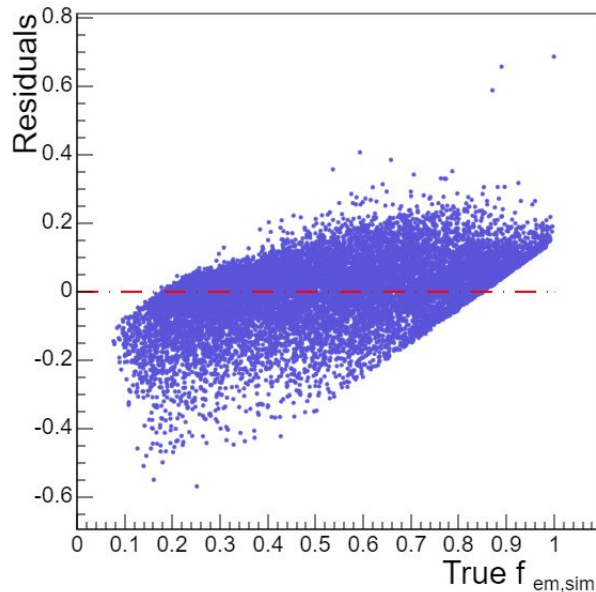
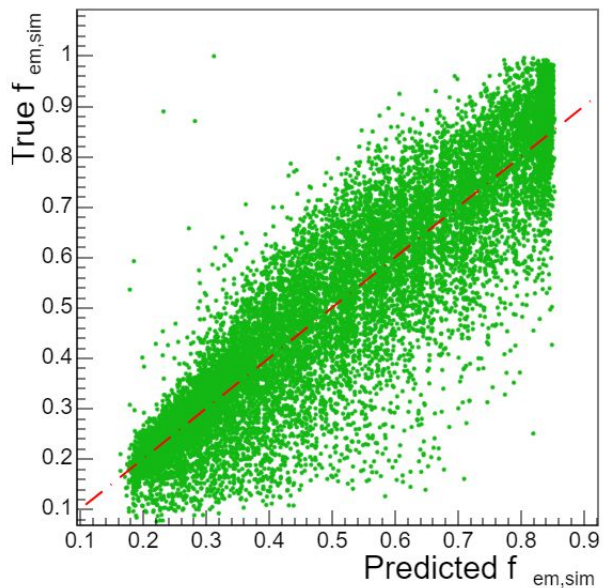
- 1. An initial model:** often a simple one like the mean of the target values for regression.
- 2. Building Trees Iteratively:** new decision trees added one at a time, each new tree trained to correct the errors or residuals of the combined ensemble of all previous trees.
- 3. Gradient Descent** to minimize a loss function.
- 4. Updating the model:** predictions from each new tree added to the ensemble model, weighted by a learning rate.
- 5. Repeat**



From: Deng, Haowen, et al., BMC Medical Informatics and Decision Making, 2021

□ Preliminary results with ML

10 GeV  $\pi^+$

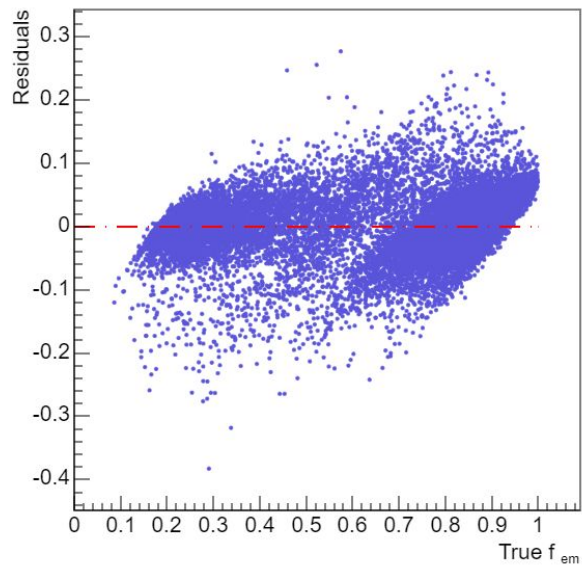
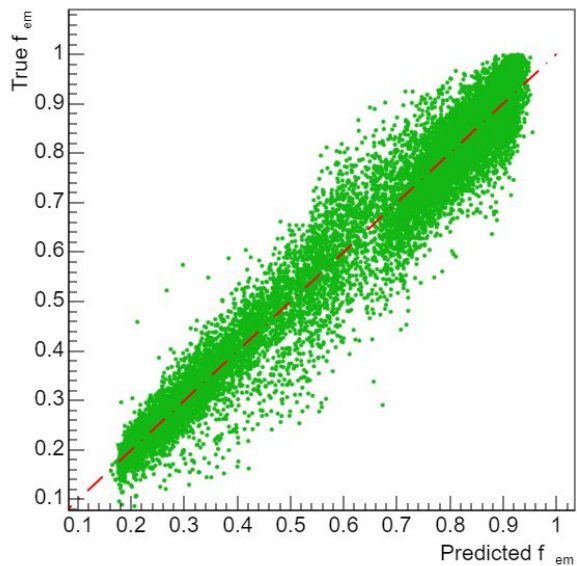


→ 33% of data for testing

→ score = 0.82

□ Preliminary results with ML

100 GeV  $\pi^+$



→ 33% of data for testing  
→ score = 0.96



## A Influence of the incident and deposited energies in the linear fit to reconstruct the deposited energy inside an ECAL

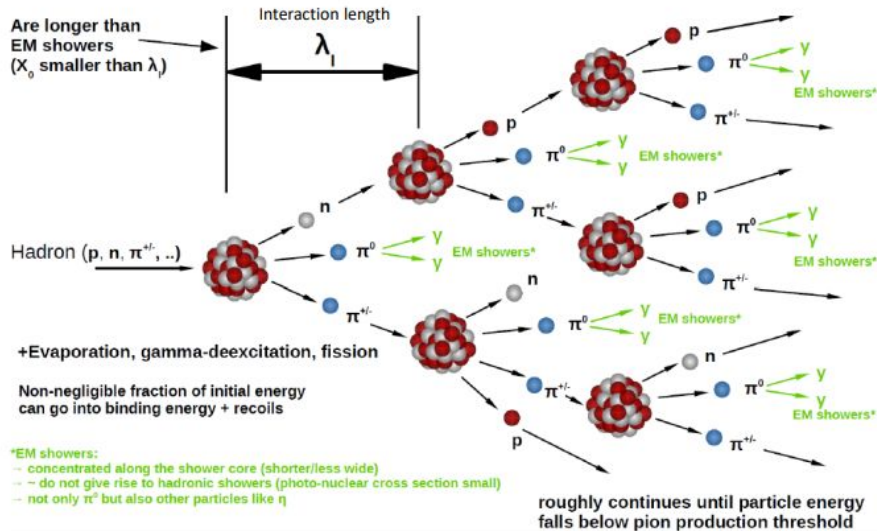
<i>Deposited energy</i> \ <i>Incident energy</i>	10	20	30	40
5	1.99 2.90	1.66 3.26	1.71 3.17	1.58 3.26
10		3.72 5.71	3.13 6.23	2.94 6.42

Table 1: Values of the linear fit to reconstruct the deposited energy for different incident energies and sections of deposited energy. The incident and deposited energy are expressed in GeV. In the cell, the first value corresponds to the slope of the fit and the second below to the constant coefficient. They are also expressed in GeV.



# Hadronic shower

## Hadronic shower scheme



2022-23

A.Besson, Université de Strasbourg

29

## Hadronic shower

- Charged Hadronic particle are slowed down by  $dE/dx$ 
  - ✓ Small effect
- In addition collision with nuclei (strong interaction)
  - ✓ Inelastic scattering: initial state  $\neq$  final state
  - ✓ At high energy:  $\sigma_I \sim 40 \text{ mb} \times A^{0.71}$
- Interaction length  $\lambda_I$ :
 

$$\lambda_I = \frac{A}{N_{Av} \rho \sigma_I}$$

which yields:  
 $N(x) = N_0 \exp(-x/\lambda_{int})$

  - ✓ e.g. Carbon:  $\rho \cdot \lambda \sim 86 \text{ g/cm}^2$
  - ✓ e.g. Lead:  $\rho \cdot \lambda \sim 194 \text{ g/cm}^2$
- $\lambda_I \gg x_0$ 
  - ✓ Hadronic showers longer than e.m. showers
- $\sim 1/3$  of the shower produces  $\pi^0 \Rightarrow$  quickly stopped by e.m. shower
- Energy threshold to produce a pion (lightest hadrons)
  - ✓ Play a similar role of  $E_c$  for electrons
  - ✓ Hadronic shower stops below this energy
- Large variety of process
  - ✓ A fraction of the energy loss can not be converted in signal
    - (nuclear binding energy, target recoil, etc.)
  - ✓ Large fluctuations in hadronic showers
  - ✓ Energy measurement less precise

2022-23

A.Besson, Université de Strasbourg

30

From: A. Besson, lectures in M2PSA 2022